saline, followed by 500 ml of 4% paraformaldehyde in 0.1 M phosphate buffer (PB; pH 7.4). The brain was quickly removed, post fixed in a solution of 4% paraformaldehyde at room temperature for 4 h, and then immersed overnight in a cold solution of 20% sucrose. Later, the brains were cut at 50 μm thickness in the frontal plane using a freezing microtome.

The immunohistochemistry procedure was carried out as described previously (Liaury et al., 2012). After incubation in 1% H_2O_2 solution, free-floating sections were preincubated with 1.5% normal goat serum and 0.2% Triton-X in 0.1 M PB (pH 7.4) for 1 h rotating at room temperature (RT), and then incubated overnight with the primary antibody, mouse anti-CD11b (1:500, AbD Serotec, Oxford, UK). Subsequently, the sections were incubated for 1 h in biotinylated anti-mouse IgG (1:200, Standard ABC Kit, Vector Labs, Burlingame, CA, USA), then incubated for 1 h in PBS containing avidin–biotin peroxidase complex (ABC). Later, the sections were developed by incubating in PBS containing 10 mg diaminobenzidine (DAB) and 5 μl of 30% hydrogen peroxide for 10 min.

For double immunofluorescent labeling, sections were incubated in the primary antibody, rabbit anti-ionized calcium binding adaptor molecule 1 (Iba1, 1:4000, Wako Ltd., Osaka, Japan), followed by Cy3-conjugated anti-rabbit IgG (1:1000, Amersham Bioscience Ltd., Piscataway, NJ, USA). For the secondary antibody, we used mouse anti-CD11b (1:500), followed by Alexa488-conjugated anti-mouse IgG (1:1000, Invitrogen, Carlsbad, CA, USA).

2.6. Measuring CD11b-labeled microglial cells immunoreactive area

The immunoreactive area was measured using a computer-assisted image analysis program (ImageTool V. 3.0, Department of Dental Diagnostic Science, University of Texas Health Science Center, San Antonio, TX, USA). Images were captured from four areas within the hippocampal DG: hilus, subgranular zone (SGZ), granular layer (GL), and molecular layer (ML). Sections containing CD11b-labeled cells were examined under a light microscope (Nikon, ECLIPSE E800). Images (N = 80 per region, per time point) were randomly captured from the same region of interest from interaural 5.88 mm, bregma −3.12 mm, to interaural 4.20 mm, bregma −4.80 mm, based on the rat brain atlas (Paxinos and Watson, 2007). The images were analyzed using the software that automates converting all immunolabeled elements that fall within a threshold range into pure black pixels and the rest of the image into pure white pixels. The software then quantifies the total numbers and percentages of black and white pixels for statistical analysis of the data.

2.7. Statistical analysis

The data are presented as the mean ± standard error of the mean (SEM). The PPI data were analyzed by three-way analysis of variance (ANOVA) using R version 3.0.2 (The R Foundation for Statistical Computing, Vienna, Austria) which analyzed the interaction between three factors (strain × treatment × prepulse intensity). When appropriate, group means at individual levels were compared by post-hoc Bonferroni analysis to determine the differences among groups. The NORT and immunohistochemistry data were analyzed by two-way ANOVA (strain × treatment) and followed by the post hoc Bonferroni test. This analysis was performed with SPSS software (Dr. SPSS II for Windows V. 11.0, SPSS Inc., Chicago, IL, USA). Significance for the result was set at $p < 0.05$.

3. Results

3.1. Effects of minocycline on PPI deficits

The PPI test was conducted with two different prepulse stimulus intensities, 70 dB and 80 dB. The three-way ANOVA revealed that there was no significant three-way interaction between strain, treatment and prepulse intensity ($F_{(1,48)} = 0.025$, $p > 0.05$). As for two-way interaction, only interaction between strain and prepulse intensity was significant ($F_{(1,48)} = 4.792$, $p < 0.05$). We found significant main effects for all factors included. The %PPI results were significantly affected by strain, treatment and prepulse intensity. %PPI was significantly lower for Gunn rats than Wistar rats ($F_{(1,48)} = 34.433$, $p < 0.001$). Treatment with minocycline produced significantly higher %PPI result than treatment with saline ($F_{(1,48)} = 4.413$, $p < 0.05$). As shown in Fig. 1, post hoc Bonferroni test revealed that the GV group had a significant lower %PPI compared to the WV group in both 70 dB ($F_{(1,24)} = 20.886$, $p < 0.001$) and 80 dB ($F_{(1,24)} = 9.040$, $p = 0.006$) tests. Treatment with minocycline for 14 days significantly increased the %PPI in the GM group compared to the GV group at 80 dB ($F_{(1,24)} = 4.360$, $p = 0.048$) but produced no significant difference at 70 dB ($F_{(1,24)} = 3.545$, $p = 0.072$). Meanwhile, no significant difference was found in WM compared to WV groups both at 70 dB ($F_{(1,24)} = 0.006$, $p = 0.941$) and at 80 dB ($F_{(1,24)} = 0.044$, $p = 0.835$).

3.2. Effects of minocycline on recognition memory

As shown in Fig. 2, in the training session, two-way ANOVA revealed that here were no significant interaction between strain × treatment in both total time ($F_{(3,38)} = 2.272$, $p = 0.913$) and in exploratory preference ($F_{(3,38)} = 2.945$, $p = 0.412$). In the retention session, two-way ANOVA revealed significant differences among the groups studied in total time ($F_{(3,38)} = 0.257$, $p = 0.005$) and in exploratory preference ($F(3,38) = 0.224$, $p = 0.004$). Post hoc analysis indicated that GV group showed significant reduction in total time ($F_{(1,38)} = 4.701$, $p = 0.036$) and exploratory preference ($F_{(1,38)} = 10.975$, $p = 0.002$) compared to the WV group. Treatment with minocycline in the GM group significantly improved the exploratory preference ($F_{(1,38)} = 8.126$, $p = 0.007$) without affecting the total exploration time ($F_{(1,38)} = 0.121$, $p = 0.730$) compared to the GV group. Meanwhile, treatment with minocycline showed no significant difference in the WM group compared to the WV group on total exploration time and exploratory preference in both the training or retention sessions.

3.3. Effects of minocycline on microglial activation

Next, we examined the effects of minocycline treatment on microglial activation in the hippocampal DG. CD11b expression in the hippocampal DG of the GV group was consistently high. In many cases, the CD11b immunoreactivity was detected not only in the thick processes, but also strongly expressed within the cell bodies of the Iba1-labeled microglial cells (Fig. 3-1b, -1c). Statistical analysis by two-way ANOVA revealed a significant interaction between strain × treatment in hilus ($F_{(3,20)} = 1.977$, $p = 0.006$), SGZ ($F_{(3,20)} = 1.902$, $p = 0.003$), granular layer ($F_{(3,20)} = 7.135$, $p = 0.045$), but not in molecule layer ($F_{(3,20)} = 6.986$, $p = 0.644$). Post hoc analysis indicated a significant increase in percentage of CD11b immunoreactivity of the GV group in the hilus ($F_{(1,20)} = 43.506$, $p < 0.001$), SGZ ($F_{(1,20)} = 57.156$, $p < 0.001$), granular layer ($F_{(1,20)} = 18.619$, $p < 0.001$), and molecular layer ($F_{(1,20)} = 11.323$, $p = 0.003$) compared to the WV group (Fig. 4a–d).

The consecutive administration of minocycline (40 mg/kg) for 14 days decreased the CD11b expression in the DG of the GM group. In this case, most CD11b immunoreactivity was expressed only on the thin ramified processes with a slight expression within the cell bodies of the Iba1-labeled microglial cells (Fig. 3-2b, 3-2c). A post hoc Bonferroni test revealed that minocycline significantly decreased the percentage of CD11b immunoreactivity in the hilus ($F_{(1,20)} = 23.510$, $p < 0.001$), SGZ ($F_{(1,20)} = 18.473$, $p < 0.001$), and granular layer ($F_{(1,20)} = 8.907$, $p = 0.007$) compared to the GV group (Fig. 4a–c). No significant difference was found between WV and WM groups.

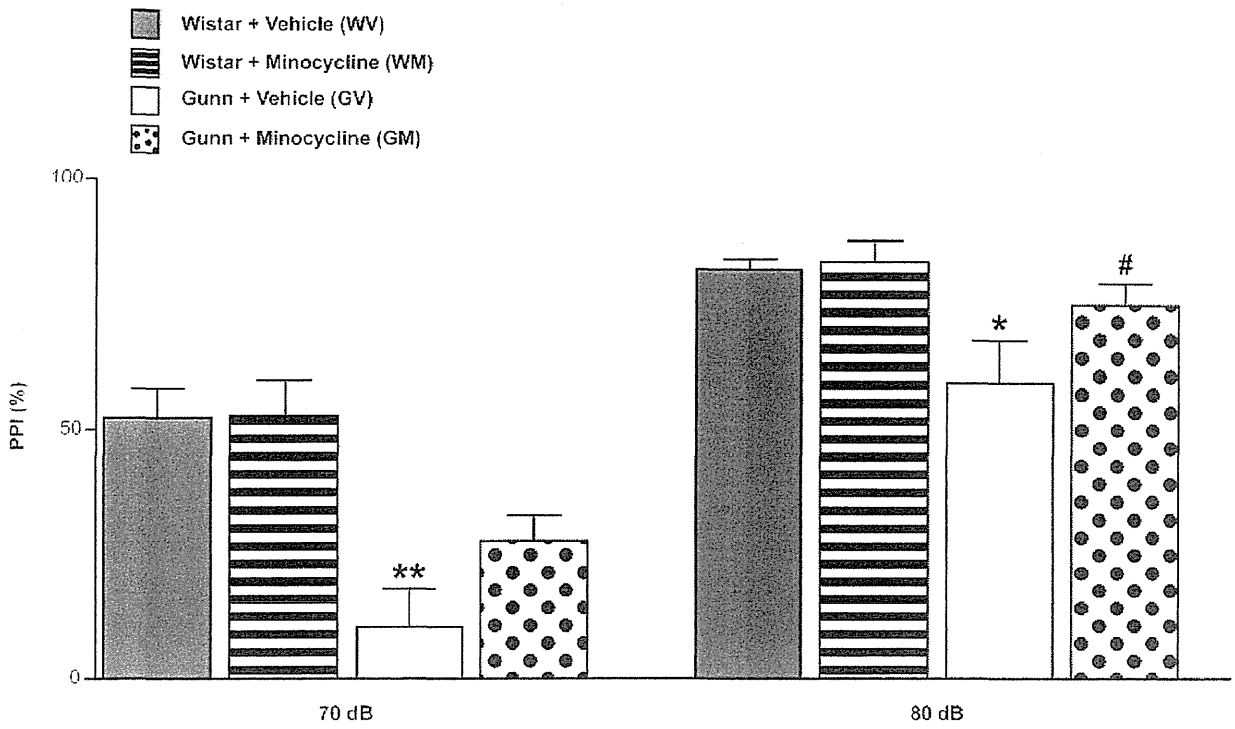

Fig. 1. Effects of minocycline on PPI test at 70 dB and 80 dB. Each value is the mean ± S.E.M. (n = 7 per group). *p < 0.01, **p < 0.001 as compared to WV control group; #p < 0.05 as compared to GV group.

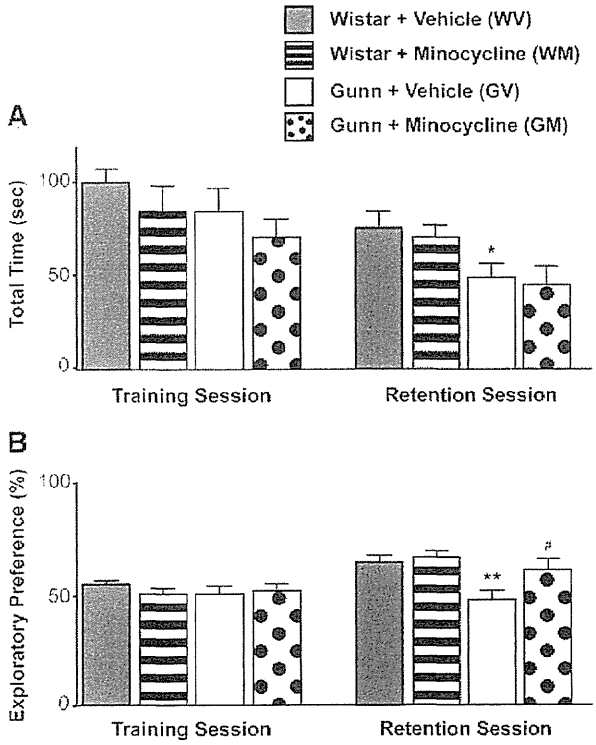

Fig. 2. Effects of minocycline on novel object recognition test (NORT). A. Total exploration time; B. exploratory preference. Each value is the mean ± S.E.M. (n = 9 each in Wistar rat group, n = 12 each in Gunn rat group). *p < 0.05, **p < 0.005 as compared to WV control group; #p < 0.01 as compared to GV group.

4. Discussion

The major findings of the present study are that minocycline significantly improved the impairment of recognition memory in Gunn rats, and that minocycline significantly attenuated the activation of microglial cells in the hippocampal DG. To our knowledge, this is the first report demonstrating the effects of minocycline on behavioral changes and on microglial activation in the Gunn rat, a possible hyperbilirubinemia-induced animal model of schizophrenia.

Our results showed that Gunn rats had lower %PPI compared to Wistar control rats, indicating that the Gunn rat has impaired sensorimotor gating. Moreover, Gunn rats also showed a reduction of exploratory preference after long-term retention interval (24 h) during NORT, indicating that the Gunn rat has impaired recognition memory. Our findings are in agreement with other animal models of schizophrenia on the association with PPI deficits (Dieckmann et al., 2007; Geyer et al., 1990) and NORT impairment (Kamei et al., 2006; Mizoguchi et al., 2008). Taking these facts together, we herein propose the Gunn rat as a potential animal model in relation to the cognitive deficits in schizophrenia.

To detect and measure the microglial activation in the hippocampal DG, we used a marker of integrin alpha M (ITGAM) cluster of differentiation molecule 11B (CD11b), which is expressed on all types of microglia, and expression of which is significantly increased on activated microglial cells (He et al., 1997). Furthermore, one of the earliest changes in microglia cells after facial nerve trisection was the up-regulation of CD11b (Graeber et al., 1988). Therefore, CD11b expression appears to be a sensitive marker of microglial activation. The hippocampal region was our main interest due to its potential role in learning and memory with the dentate gyrus (DG) as the primary gateway for inputs into the hippocampus with a continuously developing structure with birth of new neurons — 'neurogenesis' — throughout mammalian life (Gage, 2002).

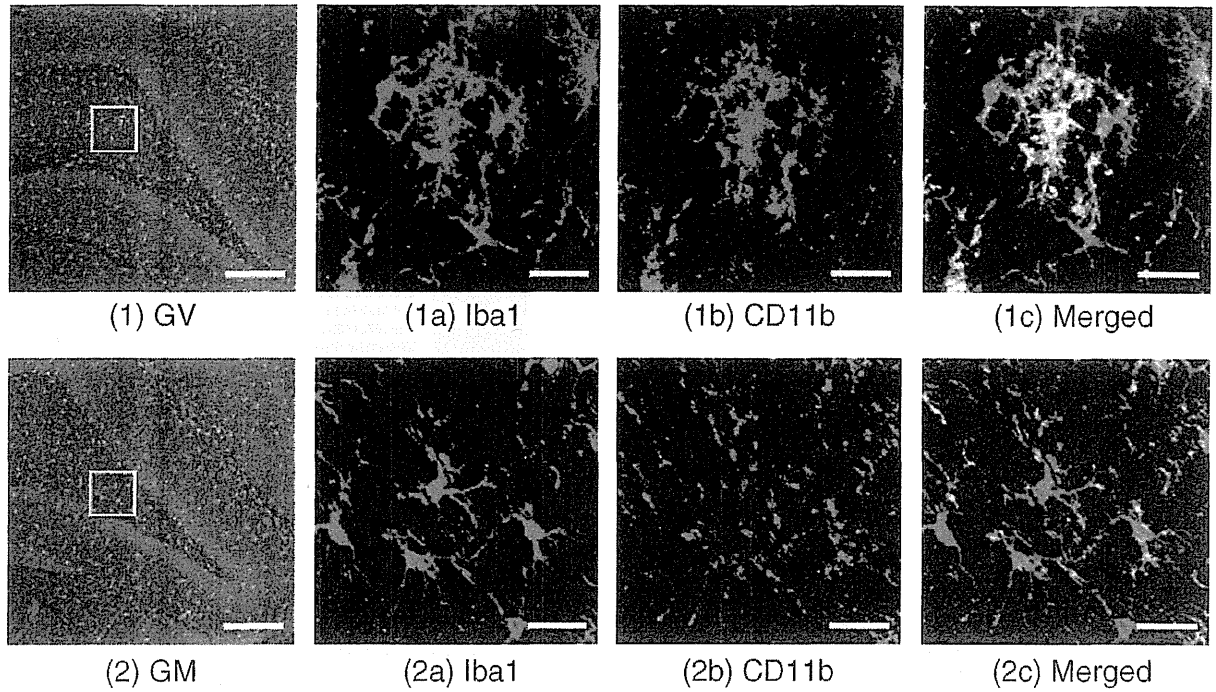

Fig. 3. CD11b expression in ionized calcium binding adaptor molecule 1 (Iba1)-labeled microglial cells. A confocal Z stack image depicting Iba1-labeled (red), CD11b expression (green), and merged (yellow) cells of vehicle-treated Gunn rat (GV) group (1a–1c) compared to those of minocycline-treated Gunn rat (GM) group. Microglial cells in the GM (2b,c) group expressed low levels of CD11b immunoreactivity compared to the GS group (1b,c). Scale bars: 200 μm (1,2), 20 μm (1a–1c, 2a–2c).

Moreover, hippocampus is also one of the brain regions whose function is altered in schizophrenia (Tamminga et al., 2010).

Consistent with our previous report, we found a significant high level of CD11b immunoreactivity in all areas of the hippocampal DG, including the hilus, SGZ, granular layer, and molecular layer in Gunn rats. The high level of CD11b immunoreactivity was accompanied by altered morphology, suggesting that microglial cells in Gunn rat were in an activated state. Microglial cell is well-known as a key player in the reaction of the cerebral innate immune system to pathological changes. Threats to CNS homeostasis can trigger a rapid transformation from a normally "ramified" state into alerted and "activated" states. Microglial cells primarily serve in tissue defense and protection when participating in the mechanisms of innate and adaptive immunity. Conversely, excessive acute or chronic microglial activation can provoke severe neuronal and glial damage by carrying or fuelling destructive cascades [for review, see (Kettenmann et al., 2011; van Rossum and Hanisch, 2004)]. Microglial cells may also contribute to synaptic modulation, learning, and memory processes. Disturbance of the functions or alterations in

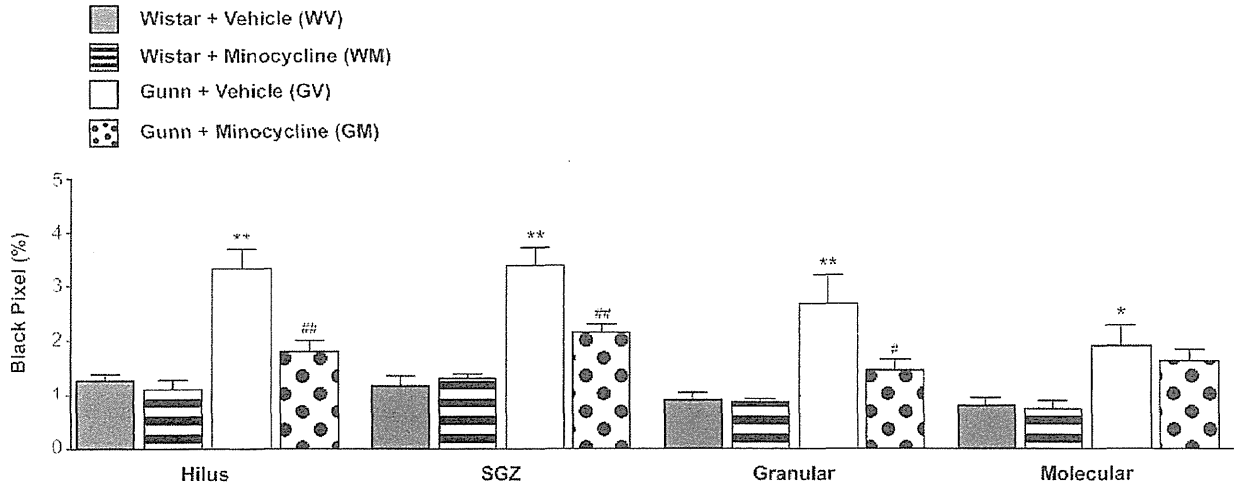

Fig. 4. Mean percentage of black pixels indicating CD11b immunoreactivity in the hippocampal dentate gyrus (DG). Each value is the mean ± S.E.M. (n = 6 per group). *$p < 0.005$, **$p < 0.001$ as compared to WV control group; #$p < 0.01$, ##$p < 0.001$ as compared to GV group.

the number and/or morphology of microglial cells in brain regions involved in cognitive and emotional aspects of behavior may represent an etiological factor in the onset or progression of memory impairment and neuropsychiatric disorders (Blank and Prinz, 2013). Accordingly, we assumed that the chronic microglial activation in adult Gunn rat is potentially more maladaptive than neuroprotective (Liaury et al., 2012), and based on our present results, we suggest that the microglial activation in the hippocampal DG in Gunn rat may be involved in promoting cognitive impairment, as was shown in the behavior test.

Consecutive administration of minocycline for 14 days significantly improved the impaired recognition memory in Gunn rats, which was indicated by the increase of exploratory preference in the retention session during NORT. Moreover, minocycline significantly attenuated the activation of microglial cells in the hippocampal DG of Gunn rats, which was indicated by the decreased immunoreactivity of CD11b marker. According to previous studies showing about the neuroprotective effects of minocycline (Miyaoka, 2012; Yrjanheikki et al., 1998), we assume that this phenomenon is part of the mechanism underlying minocycline's anti-inflammatory properties through inhibition of microglial activation. Similar results were reported that minocycline significantly improved the recognition memory of mice treated with methamphetamine (Mizoguchi et al., 2008) and phencyclidine (Fujita et al., 2008). Minocycline was also reported to significantly attenuate the microglial activation in mouse brains induced by methamphetamine and 3,4-methylenedioxymethamphetamine (Zhang et al., 2006a, 2006b). Taking these facts and our results into consideration, we speculate that the inhibition of microglial activation by minocycline in the hippocampal DG may, in part, be implicated in the mechanism of minocycline action to improve the recognition memory in Gunn rats. Although we demonstrated that minocycline attenuated microglial activation, we did not evaluate its effects on inflammatory markers, such as pro-inflammatory cytokines and chemokines. Therefore, it may be of interest to further study and establish the anti-inflammatory effects of minocycline in Gunn rats. On the other hand, the PPI deficit in Gunn rats was not fully rescued by minocycline administration. While the results at the 80 dB showed a significant improvement in the PPI deficits, later we only found a tendency toward improvement at the 70 dB. We speculate that this may be due to the small number of animals used for the PPI test ($n = 7$, per group). Other possibility is that it may be due to the incomplete inhibition of microglial activation, since minocycline did not reduce the immunoreactivity of CD11b in the molecular layer of the hippocampal DG in Gunn rats. Another study also reported the partial improvement of minocycline on olfactory bulbectomized (OBX) rats, a model of cognitive and behavioral impairments arising from neurodegenerative processes (Borre et al., 2012). Minocycline normalized OBX-induced hyperactivity in the open field, protected against hippocampal dependent spatial memory deficit, but failed to prevent fear memory loss. They suggested that minocycline may have ameliorated the OBX-induced cognitive deficits in a region specific manner and that treatment with minocycline may be effective in the early phase of a neurodegenerative disease.

However, the exact cellular and molecular mechanisms underlying this complex UCB–neuron–glia interaction in Gunn rats still remain elusive. We presume that another mechanism may also be involved, which is mediated through the glutamatergic system in the brain. Exposure of glia cells to UCB increases the extracellular concentration of glutamate by decreased uptake (Silva et al., 1999) and/or enhanced secretion (Fernandes et al., 2004), engendering overstimulation of glutamate and N-methyl-D-aspartate (NMDA) receptor (Ostrow et al., 2004). Moreover, high levels of bilirubin can lower the brain's threshold and enhance its vulnerability to NMDA-triggered excitotoxic brain injury (McDonald et al., 1998). Release of pro-inflammatory cytokines may affect gliogenesis and neurogenesis, and may lead to deficits in learning and memory. Dysregulation of glutamate metabolism and over-expression of tumor necrosis factor-α (TNF-α) and interleukin (IL)-1β are consistent with schizophrenia neuropathology. Increased proinflammatory status of the brain also interacts with glutamatergic and dopaminergic neurotransmission, which can induce or aggravate positive, negative, and cognitive symptoms of schizophrenia (Muller and Schwarz, 2006). Interestingly, some studies have shown that minocycline has properties that affect glutamatergic pathways. Administration of minocycline to neurons in-vitro and to mice in-vivo increased GluR1 phosphorylation and membrane insertion (Imbesi et al., 2008). GluR1 receptors, which appear to be critical for cognitive processes that are impaired in schizophrenia, may be crucially involved in the pathobiology of schizophrenia (Wiedholz et al., 2008). Moreover, minocycline attenuated behavioral changes after administration of a non-competitive N-methyl-D-aspartate (NMDA) receptor antagonist (Levkovitz et al., 2007; Zhang et al., 2007).

Inhibition of chronic neuroinflammation, particularly of microglial activation, has been suggested to be a practical strategy in the treatment of many psychiatry diseases, including schizophrenia (Dean et al., 2012). Two studies reported the effectiveness of minocycline adjunctive therapy in early schizophrenia for negative symptoms (Chaudhry et al., 2012; Levkovitz et al., 2010). In addition, Levkovitz et al. also reported the improvement on cognitive function. Another report showed two cases with persistent schizophrenia symptoms despite long term clozapine treatment that were treated successfully with adjunct minocyline (Kelly et al., 2011). Moreover, long term treatment with minocycline is generally safe and well tolerated in humans (Bonelli et al., 2003; Stone et al., 2003). Taken together, it might be worthwhile to further explore the effects of minocycline in schizophrenia.

5. Conclusion

The present study indicates that minocycline improves recognition memory and attenuates the activation of microglial cells in the hippocampal DG of Gunn rat, a possible hyperbilirubinemia-induced animal model of schizophrenia. Therefore, minocycline may be a potential therapeutic drug for schizophrenia. Our results may also provide crucial information to elucidate the etiology of schizophrenia and support the possibility of using the Gunn rat as an animal model of schizophrenia.

Acknowledgments

This work was supported in part by a Grant-in-Aid for Scientific Research (C) (No. 13201342) from the Ministry of Education, Culture, Sports, Science, and Technology of Japan, and by a Health and Labor Sciences Research Grant for Clinical Research (No. 04T-580) from the Ministry of Health, Labor, and Welfare of Japan. Part of KL's work was also supported by a grant from the Hashiya Scholarship Foundation. All authors have read and approved the final manuscript. The authors declare no competing interest. We thank Dr. Hideaki Yasuda (Department of Psychiatry, Shimane University Faculty of Medicine) and Akira Yasuda (Department of Medical Biostatistic, Shimane University Faculty of Medicine) for their valuable suggestions on statistical analysis. We are particularly grateful to Katherine Ono for editorial assistance.

References

Bian Q, Kato T, Monji A, Hashioka S, Mizoguchi Y, Horikawa H, et al. The effect of atypical antipsychotics, perospirone, ziprasidone and quetiapine on microglial activation induced by interferon-gamma. Prog Neuropsychopharmacol Biol Psychiatry 2008;32(1):42–8.

Blank T, Prinz M. Microglia as modulators of cognition and neuropsychiatric disorders. Glia 2013;61(1):62–70.

Bonelli RM, Heuberger C, Reisecker F. Minocycline for Huntington's disease: an open label study. Neurology 2003;60(5):883–4.

Borre Y, Sir V, de Kivit S, Westphal KG, Olivier B, Oosting RS. Minocycline restores spatial but not fear memory in olfactory bulbectomized rats. Eur J Pharmacol 2012;697(1–3):59–64.

Chaudhry IB, Hallak J, Husain N, Minhas F, Stirling J, Richardson P, et al. Minocycline benefits negative symptoms in early schizophrenia: a randomised double-blind placebo-controlled clinical trial in patients on standard treatment. J Psychopharmacol 2012;26(9):1185–93.

Dean OM, Data-Franco J, Giorlando F, Berk M. Minocycline: therapeutic potential in psychiatry. CNS Drugs 2012;26(5):391–401.
Dieckmann M, Freudenberg F, Klein S, Koch M, Schwabe K. Disturbed social behavior and motivation in rats selectively bred for deficient sensorimotor gating. Schizophr Res 2007;97(1–3):250–3.
Doorduin J, de Vries EF, Willemsen AT, de Groot JC, Dierckx RA, Klein HC. Neuroinflammation in schizophrenia-related psychosis: a PET study. J Nucl Med 2009;50(11):1801–7.
Erbagci AB, Herken H, Koyluoglu O, Yilmaz N, Tarakcioglu M. Serum IL-1beta, sIL-2R, IL-6, IL-8 and TNF-alpha in schizophrenic patients, relation with symptomatology and responsiveness to risperidone treatment. Mediators Inflamm 2001;10(3):109–15.
Fernandes A, Silva RF, Falcao AS, Brito MA, Brites D. Cytokine production, glutamate release and cell death in rat cultured astrocytes treated with unconjugated bilirubin and LPS. J Neuroimmunol 2004;153(1–2):64–75.
Ferretti MT, Allard S, Partridge V, Ducatenzeiler A, Cuello AC. Minocycline corrects early, pre-plaque neuroinflammation and inhibits BACE-1 in a transgenic model of Alzheimer's disease-like amyloid pathology. J Neuroinflammation 2012;9(62):1742–2094.
Fisman M. The brain stem in psychosis. Br J Psychiatry 1975;126:414–22.
Fujita Y, Ishima T, Kunitachi S, Hagiwara H, Zhang L, Iyo M, et al. Phencyclidine-induced cognitive deficits in mice are improved by subsequent subchronic administration of the antibiotic drug minocycline. Prog Neuropsychopharmacol Biol Psychiatry 2008;32(2):336–9.
Gage FH. Neurogenesis in the adult brain. J Neurosci 2002;22(3):612–3. [2002 Feb 1].
Geyer MA, Swerdlow NR, Mansbach RS, Braff DL. Startle response models of sensorimotor gating and habituation deficits in schizophrenia. Brain Res Bull 1990;25(3):485–98.
Graeber MB, Streit WJ, Kreutzberg GW. Axotomy of the rat facial nerve leads to increased CR3 complement receptor expression by activated microglial cells. J Neurosci Res 1988;21(1):18–24.
Gunn CK. Hereditary acholuric jaundice in the rat. Can Med Assoc J 1944;50(3):230–7.
Hayashida M, Miyaoka T, Tsuchie K, Yasuda H, Wake R, Nishida A, et al. Hyperbilirubinemia-related behavioral and neuropathological changes in rats: a possible schizophrenia animal model. Prog Neuropsychopharmacol Biol Psychiatry 2009;33(4):581–8.
Ho BP, Tay SS, Leong SK. Microglia responses in the CNS following sciatic nerve transection in C57BL Wld(s) and BALB/c mice. Exp Neurol 1997;146(2):587–95.
Imbesi M, Uz T, Manev R, Sharma RP, Manev H. Minocycline increases phosphorylation and membrane insertion of neuronal GluR1 receptors. Neurosci Lett 2008;447(2–3):134–7.
Jacobi G, Mantz MP, Brune M, Friebe A, Heneka MT, Wolf RJ. Microglial activation in a neuroinflammational animal model of schizophrenia – a pilot study. Schizophr Res 2011;131(1–3):96–100.
Kamei H, Nagai T, Nakano H, Togan Y, Takayanagi M, Takahashi K, et al. Repeated methamphetamine treatment impairs recognition memory through a failure of novelty-induced ERK1/2 activation in the prefrontal cortex of mice. Biol Psychiatry 2006;59(1):67–74.
Kato T, Monji A, Hashioka S, Kanba S. Risperidone significantly inhibits interferon-gamma-induced microglial activation in vitro. Schizophr Res 2007;92(1–3):108–15.
Kelly DL, Vyas G, Richardson CM, Koola M, McMahon RP, Buchanan RW, et al. Adjunct minocycline to clozapine treated patients with persistent schizophrenia symptoms. Schizophr Res 2011;133(1–3):257–8. http://dx.doi.org/10.1016/j.schres.2011.08.005. [2011 Dec, Epub 2011 Aug 26].
Kettenmann H, Hanisch UK, Koda M, Verkhratsky A. Physiology of microglia. Physiol Rev 2011;91(2):461–553.
Kneeland RE, Fatemi SH. Viral infection, inflammation and schizophrenia. Prog Neuropsychopharmacol Biol Psychiatry 2013;42:35–48.
Laan W, Grobbee DE, Selten JP, Heijnen CJ, Kahn RS, Burger H. Adjuvant aspirin therapy reduces symptoms of schizophrenia spectrum disorders: results from a randomized, double-blind, placebo-controlled trial. J Clin Psychiatry 2010;71(5):520–7.
Levkovitz Y, Levi H, Braw Y, Cohen H. Minocycline, a second-generation tetracycline, as a neuroprotective agent in an animal model of schizophrenia. Brain Res 2007;18:154–62.
Levkovitz Y, Mendlovich S, Riwkes S, Braw Y, Levkovitch-Verbin H, Gal G, et al. A double-blind, randomized study of minocycline for the treatment of negative and cognitive symptoms in early-phase schizophrenia. J Clin Psychiatry 2010;71(2):138–49.
Liaury K, Miyaoka T, Tsumori T, Furuya M, Wake R, Ieda M, et al. Morphological features of microglial cells in the hippocampal dentate gyrus of Gunn rat: a possible schizophrenia animal model. J Neuroinflammation 2012;9(56):1742–2094.
McDonald JW, Shapiro SM, Silverstein FS, Johnston MV. Role of glutamate receptor-mediated excitotoxicity in bilirubin-induced brain injury in the Gunn rat model. Exp Neurol 1998;150(1):21–9.
Mednick SA, Machon RA, Huttunen MO, Bonett D. Adult schizophrenia following prenatal exposure to an influenza epidemic. Arch Gen Psychiatry 1988;45(2):189–92.
Meyer U. Developmental neuroinflammation and schizophrenia. Prog Neuropsychopharmacol Biol Psychiatry 2013;42:20–34.
Miller BJ, Buckley P, Seabolt W, Mellor A, Kirkpatrick B. Meta-analysis of cytokine alterations in schizophrenia: clinical status and antipsychotic effects. Biol Psychiatry 2011;70(7):663–71.
Miller BJ, Culpepper N, Rapaport MH, Buckley P. Prenatal inflammation and neurodevelopment in schizophrenia: a review of human studies. Prog Neuropsychopharmacol Biol Psychiatry 2013;42:92–100.
Miyaoka T. Minocycline for schizophrenia: a critical review. Open J Psychiatry 2012;2:399–406.
Miyaoka T, Yasukawa R, Yasuda H, Hayashida M, Inagaki T, Horiguchi J. Possible antipsychotic effects of minocycline in patients with schizophrenia. Prog Neuropsychopharmacol Biol Psychiatry 2007;31(1):304–7.
Miyaoka T, Yasukawa R, Yasuda H, Hayashida M, Inagaki T, Horiguchi J. Minocycline as adjunctive therapy for schizophrenia: an open-label study. Clin Neuropharmacol 2008;31(5):287–92.
Mizoguchi H, Takuma K, Fukakusa A, Ito Y, Nakatani A, Ibi D, et al. Improvement by minocycline of methamphetamine-induced impairment of recognition memory in mice. Psychopharmacology (Berl) 2008;196(2):233–41.
Muller N, Schwarz M. Schizophrenia as an inflammation-mediated dysbalance of glutamatergic neurotransmission. Neurotox Res 2006;10(2):131–48.
Muller N, Schwarz MJ. COX-2 inhibition in schizophrenia and major depression. Curr Pharm Des 2008;14(14):1452–65.
Ostrow JD, Pascolo L, Brites D, Tiribelli C. Molecular basis of bilirubin-induced neurotoxicity. Trends Mol Med 2004;10(2):65–70.
Paxinos G, Watson C. The rat brain in stereotaxic coordinates. London: Elsevier Inc.; 2007 [Vol 6th Edition].
Radewicz K, Garey LJ, Gentleman SM, Reynolds R. Increase in HLA-DR immunoreactive microglia in frontal and temporal cortex of chronic schizophrenics. J Neuropathol Exp Neurol 2000;59(2):137–50.
Ripke S, Sanders AR, Kendler KS, Levinson DF, Sklar P, Holmans PA, et al. Genome-wide association study identifies five new schizophrenia loci. Nat Genet 2011;43(10):969–76.
Schwab SG, Hallmayer J, Freimann J, Lerer B, Albus M, Borrmann-Hassenbach M, et al. Investigation of linkage and association/linkage disequilibrium of HLA A-, DQA1-, DQB1-, and DRB1- alleles in 69 sib-pair- and 89 trio-families with schizophrenia. Am J Med Genet 2002;114(3):315–20.
Silva R, Mata LR, Gulbenkian S, Brito MA, Tiribelli C, Brites D. Inhibition of glutamate uptake by unconjugated bilirubin in cultured cortical rat astrocytes: role of concentration and pH. Biochem Biophys Res Commun 1999;265(1):67–72.
Steiner J, Bielau H, Brisch R, Danos P, Ullrich O, Mawrin C, et al. Immunological aspects in the neurobiology of suicide: elevated microglial density in schizophrenia and depression is associated with suicide. J Psychiatr Res 2008;42(2):151–7.
Stone M, Fortin PR, Pacheco-Tena C, Inman RD. Should tetracycline treatment be used more extensively for rheumatoid arthritis? Metaanalysis demonstrates clinical benefit with reduction in disease activity. J Rheumatol 2003;30(10):2112–22.
Takahashi N, Sakurai T. Roles of glial cells in schizophrenia: possible targets for therapeutic approaches. Neurobiol Dis 2013;53:49–60.
Tamminga CA, Stan AD, Wagner AD. The hippocampal formation in schizophrenia. Am J Psychiatry 2010;167(10):1178–93.
Tsuchie K, Miyaoka T, Furuya M, Liaury K, Ieda M, Wake R, et al. The effects of antipsychotics on behavioral abnormalities of the Gunn rat (unconjugated hyperbilirubinemia rat), a rat model of schizophrenia. Asian Journal of Psychiatry 2013;6(2):119–23.
van Berckel BN, Bossong MG, Boellaard R, Kloet R, Schuitemaker A, Caspers E, et al. Microglia activation in recent-onset schizophrenia: a quantitative (R)-[^{11}C]PK11195 positron emission tomography study. Biol Psychiatry 2008;64(9):820–2.
van Os J, Kapur S. Schizophrenia. Lancet 2009;374(9690):635–45.
van Rossum D, Hanisch UK. Microglia. Metab Brain Dis 2004;19(3–4):393–411.
Wiedholz LM, Owens WA, Horton RE, Feyder M, Karlsson RM, Hefner K, et al. Mice lacking the AMPA GluR1 receptor exhibit striatal hyperdopaminergia and 'schizophrenia-related' behaviors. Mol Psychiatry 2008;13(6):631–40.
Yrjanheikki J, Keinanen R, Pellikka M, Hokfelt T, Koistinaho J. Tetracyclines inhibit microglial activation and are neuroprotective in global brain ischemia. Proc Natl Acad Sci U S A 1998;95(26):15769–74.
Zhang L, Kitaichi K, Fujimoto Y, Nakayama H, Shimizu E, Iyo M, et al. Protective effects of minocycline on behavioral changes and neurotoxicity in mice after administration of methamphetamine. Prog Neuropsychopharmacol Biol Psychiatry 2006a;30(8):1381–93.
Zhang L, Shirayama Y, Shimizu E, Iyo M, Hashimoto K. Protective effects of minocycline on 3,4-methylenedioxymethamphetamine-induced neurotoxicity in serotonergic and dopaminergic neurons of mouse brain. Eur J Pharmacol 2006b;544(1–3):1–9.
Zhang L, Shirayama Y, Iyo M, Hashimoto K. Minocycline attenuates hyperlocomotion and prepulse inhibition deficits in mice after administration of the NMDA receptor antagonist dizocilpine. Neuropsychopharmacology 2007;32(9):2004–10.

Tanigawa et al. BMC Complementary and Alternative Medicine 2014, 14:133
http://www.biomedcentral.com/1472-6882/14/133

BMC
Complementary & Alternative Medicine

RESEARCH ARTICLE Open Access

(+)-Catechin protects dermal fibroblasts against oxidative stress-induced apoptosis

Tomoko Tanigawa[1], Shigeyuki Kanazawa[1*], Ryoko Ichibori[1], Takashi Fujiwara[1], Takuya Magome[2], Kenta Shingaki[3], Shingo Miyata[4], Yuki Hata[1], Koichi Tomita[1], Ken Matsuda[5], Tateki Kubo[1], Masaya Tohyama[3], Kenji Yano[1] and Ko Hosokawa[1]

Abstract

Background: Oxidative stress has been suggested as a mechanism underlying skin aging, as it triggers apoptosis in various cell types, including fibroblasts, which play important roles in the preservation of healthy, youthful skin. Catechins, which are antioxidants contained in green tea, exert various actions such as anti-inflammatory, anti-bacterial, and anti-cancer actions. In this study, we investigated the effect of (+)-catechin on apoptosis induced by oxidative stress in fibroblasts.

Methods: Fibroblasts (NIH3T3) under oxidative stress induced by hydrogen peroxide (0.1 mM) were treated with either vehicle or (+)-catechin (0–100 μM). The effect of (+)-catechin on cell viability, apoptosis, phosphorylation of c-Jun terminal kinases (JNK) and p38, and activation of caspase-3 in fibroblasts under oxidative stress were evaluated.

Results: Hydrogen peroxide induced apoptotic cell death in fibroblasts, accompanied by induction of phosphorylation of JNK and p38 and activation of caspase-3. Pretreatment of the fibroblasts with (+)-catechin inhibited hydrogen peroxide-induced apoptosis and reduced phosphorylation of JNK and p38 and activation of caspase-3.

Conclusion: (+)-Catechin protects against oxidative stress-induced cell death in fibroblasts, possibly by inhibiting phosphorylation of p38 and JNK. These results suggest that (+)-catechin has potential as a therapeutic agent for the prevention of skin aging.

Keywords: Catechin, Fibroblast, Apoptosis, Oxidative stress

Background

Skin wrinkles and sagging are important factors defining skin youthfulness. Development of methods to reduce skin wrinkles and prevent sagging skin has become an important research topic in aesthetic and anti-aging medicine. Skin wrinkles and sagging are reported to be influenced by the amount of collagen, elastin, and hyaluronic acid [1]. Fibroblasts play a key role in the production of these extracellular matrix components in the skin. Skin aging is the consequence of reduced numbers of fibroblasts, lower levels of extracellular matrix proteins, and decreased skin elasticity and tonus, thereby resulting in the formation of wrinkles [2]. Therefore, maintaining the population of dermal fibroblasts is important for both preventing and treating age-related skin changes.

Oxidative stress has been indicated in a variety of pathological processes, such as atherosclerosis, diabetes, neurodegenerative diseases, and aging. Reactive oxygen species induce DNA damage, intracellular lipid peroxidation, and abnormal protein oxidation reactions, all of which result in cell damage. Oxidative stress also promotes skin aging [3]; it reduces the number of skin fibroblasts by inducing apoptosis and decreasing their regenerative capacity, which in turn leads to increased skin sagging. Therefore, suppression of oxidative stress-induced apoptosis in skin fibroblasts is a potential treatment and prevention strategy for maintaining healthy youthful skin.

Green tea, which is routinely consumed in Japan and China, is widely known as a healthy drink containing various antioxidants, vitamins, and minerals. Catechins, including (−)-epigallocatechin gallate (EGCG), (−)-epigallocatechin

* Correspondence: kanazawa@psurg.med.osaka-u.ac.jp
[1]Department of Plastic Surgery, Osaka University Graduate School of Medicine, Suita-shi, Osaka, Japan
Full list of author information is available at the end of the article

(EGC), (−)-epicatechin gallate (ECG), and (−)-epicatechin (EC) (Figure 1), account for approximately 10% of the dry weight of green tea leaves. Catechins are thought to not only possess antioxidant effects to control active oxygen [4-7] but also exert various actions, such as anti-inflammatory [8], antibacterial [9,10], and anti-cancer [11-13] actions.

In this study, we demonstrate that (+)-catechin has an inhibitory effect against oxidative stress-induced apoptosis in fibroblasts, accompanied by suppression of phosphorylation of p38 and c-Jun terminal kinases (JNK), both of which play an important role in intracellular apoptotic signaling induced by oxidative stress.

Methods

Cell culture

NIH 3T3 fibroblasts were used for all experiments. Cells were cultured in Dulbecco's Modified Eagle Medium (DMEM; Life Technologies CA, USA) containing 10% fetal bovine serum (FBS), 100 U/ml penicillin, and 100 μg/ml streptomycin (Life Technologies) in a humidified incubator at 37°C with 5% CO_2. All experiments were performed in triplicate.

Cell viability assay

Cell survival was determined using the 3-(4,5-dimethylthiazole-2-yl)-2,5-diphenyltetrazolium bromide (MTT) assay (CellTiter 96® AQueous One Solution Cell Proliferation Assay; Promega, WI, USA). Fibroblasts were plated at a density of 5,000 cells per well on 96-well plates and incubated for 24 h in 100 μl of DMEM containing 10% FBS. After incubation with serum-free medium for 24 h, cells were treated for 30 min with various concentrations of (+)-catechin (0–400 μM; Sigma Aldrich, PA, USA), and then subjected to oxidative stress induction with 0.1 mM hydrogen peroxide (H_2O_2). After 24 h, 20 μl of One Solution Reagent was added into each well and incubated at 37°C for 2 h in a humidified, 5% CO_2 atmosphere. The production of formazan by viable cells was detected by measuring the absorbance at 490 nm using a 96-well plate reader.

Another series of experiments were conducted to compare cytotoxicity between (+)-catechin and EGCG. Fibroblasts were treated with various concentrations of (+)-catechin or EGCG (0–400 μM; Sigma Aldrich) without H_2O_2 for 24 h and the cells were then subjected to MTT assay.

TUNEL staining

Apoptosis was determined by terminal deoxynucleotidyl transferase (TdT)-mediated dUTP-biotin nick end labeling (TUNEL) using the *In Situ* Cell Death Detection Kit TMR Red (Roche, Mannheim, Germany), according to

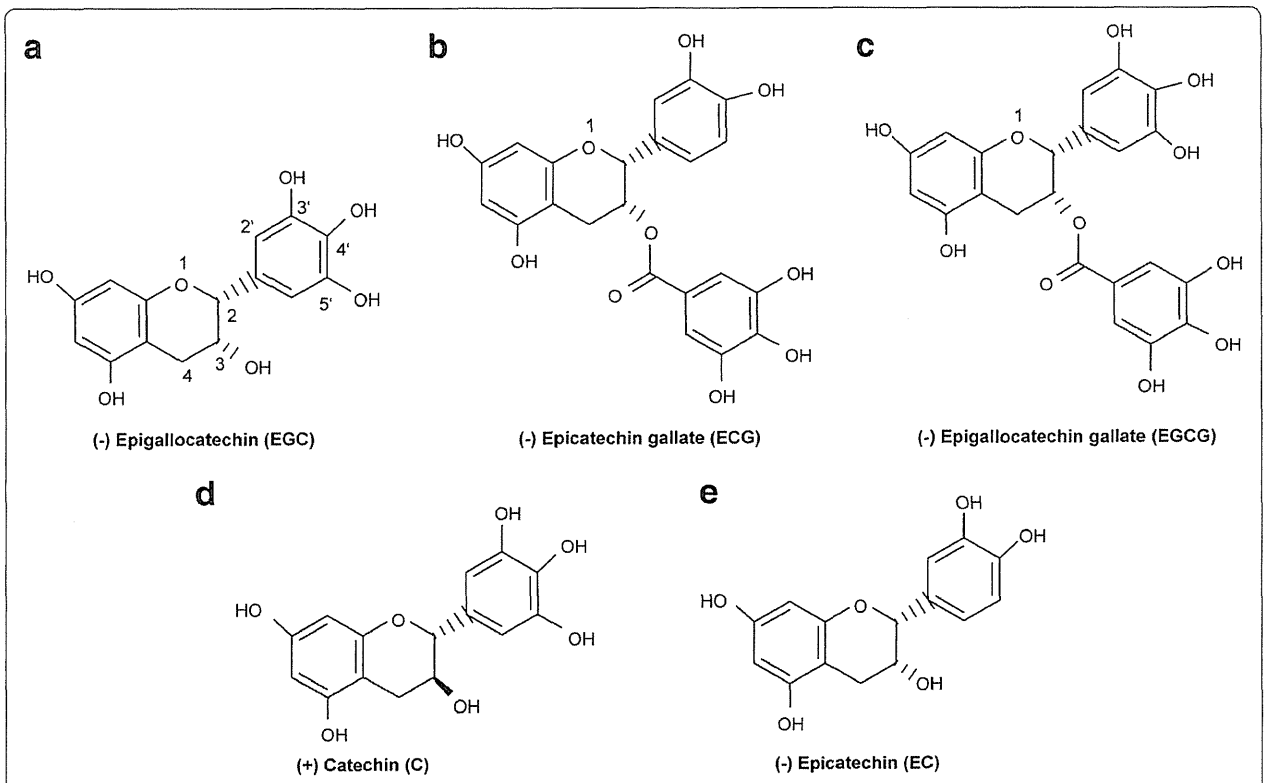

Figure 1 Chemical Structures of catechins. Structures of (−)-epigallocatechin (EGC) **(a)**, (−)-epicatechin gallate (ECG) **(b)**, (−)-epigallocatechin gallate (EGCG) **(c)**, (+)-catechin(C) **(d)**, and (−)-epicatechin (EC) **(e)**.

the manufacturer's instructions. In brief, fibroblasts were maintained in DMEM containing 10% FBS for 2 days and then cultured in serum-free DMEM. Oxidative stress was induced by addition of 0.1 mM H_2O_2 prior to treatment with 10 μM (+)-catechin or vehicle. After 24 h of incubation with H_2O_2 and (+)-catechin or vehicle, cells were fixed with 4% paraformaldehyde in phosphate-buffered saline (PBS) (pH 7.4) for 60 min at room temperature, followed by five washes with PBS. Next, permeabilization was performed by incubation with 0.1% Triton X-100 in PBS for 10 min, and cells were mixed with TUNEL reaction mixtures containing TdT and tetramethylrhodamine (TMR) red-labeled nucleotides for 1 h. Coverslips were mounted onto slides using VECTASHIELD Mounting Medium with 4′,6-diamidino-2-phenylindole dihydrochloride (Vector Laboratories, Peterborough, England). Fluorescence images were taken using a microscope (IX-70; Olympus) equipped with a charge-coupled device camera (CoolSNAP HQ; Nippon Roper, Chiba, Japan). For each experiment, 100 cells were randomly selected, and the percentage of TUNEL-positive cells was measured.

Western blot analysis

Cultured fibroblasts were serum-starved for 24 h in serum-free DMEM and then incubated with 10 μM (+)-catechin for 30 min prior to oxidative stress induction by 0.1 mM H_2O_2. After H_2O_2 challenge for 1 h, cells were harvested and lysed in radioimmunoprecipitation assay buffer containing 1 mM Na_3VO_4, 1 mM NaF, and Protease Inhibitor Cocktail (Roche Diagnostics, Basel, Switzerland) for 20 min at 4°C. After centrifugation at 15,000 × *g* for 15 min at 4°C, proteins were separated by sodium dodecyl sulfate-polyacrylamide gel electrophoresis and transferred onto Immobilon-P Transfer Membranes (Millipore Japan, Tokyo, Japan). Membranes were incubated for 60 min in Tris-buffered saline containing 5% skim milk and 0.05% Tween-20 and then blotted with the following primary antibodies at 4°C overnight: anti-phospho-JNK (1:1,000), anti-JNK (1:1,000), anti-phospho-p38 (1:1,000), anti-p38 (1:1,000), anti-cleaved caspase-3 (1:200), and anti-caspase-3 antibodies (1:200). All antibodies were purchased from Cell Signaling Technology, MA, USA. Next, membranes were incubated for 1 h with an anti-mouse or anti-rabbit HRP-linked secondary antibody (1:2,000; Cell Signaling Technology). Reaction products were visualized by chemiluminescence detection using the ECL Western Blotting Detection System (GE Healthcare, Piscataway, NJ, USA). Quantification of relative band densities was performed by densitometry using Image J software (National Institutes of Health, Bethesda, MD, USA).

Statistical analysis

All data shown are expressed as the mean ± SE of three independent experiments. Data from each experiment were normalized to the respective control sample. Differences between conditions were analyzed by Student's *t* test. Multiple-group comparisons were performed using a one-way analysis of variance, followed by Tukey's post hoc test. $P < 0.05$ was considered statistically significant.

Results

Catechin increases the viability of fibroblasts

Oxidative stress is known to promote fibroblast cell death [14]. To analyze the effect of (+)-catechin on the viability of fibroblasts in response to oxidative stress, cells cultured with various concentrations (0–100 μM) of catechin were subjected to oxidative stress induction by 0.1 mM H_2O_2. The cell numbers were analyzed after 24 h. Microscopic observation and MTT assay showed that H_2O_2 induced-oxidative stress reduced cell viability, whereas (+)-catechin suppressed the effect of H_2O_2-induced oxidative stress on cell viability in a concentration-dependent manner (Figure 2a-c).

As shown in Figure 3, microscopic evaluation of the morphological changes showed that H_2O_2 supplementation in the culture media induced apoptotic cell death characterized by shrinkage of the cell body, whereas treatment with (+)-catechin attenuated H_2O_2-induced cell death.

(+)-Catechin inhibits oxidative stress-induced apoptosis in fibroblasts

To determine whether (+)-catechin has an inhibitory effect on oxidative stress-induced apoptosis in fibroblasts, we assessed the apoptosis of fibroblasts in either the presence or absence of (+)-catechin by TUNEL staining. (+)-Catechin (10 μM)-treated fibroblasts showed significant decreases in the percentage of cells positive for TUNEL staining, compared to vehicle-treated cells (9.14% ± 0.6% vs. 1.86% ± 0.3%; Figure 4).

Effect of catechin on the activation of caspase-3 by H_2O_2-induced oxidative stress in fibroblasts

Western blotting analysis using an anti-cleaved caspase-3 antibody showed that the level of cleaved caspase-3 induced by H_2O_2 was reduced by treatment with 10 μM (+)-catechin (Figure 5). These results suggest that (+)-catechin inhibits caspase-3-dependent apoptosis induced by oxidative stress in fibroblasts.

(+)-Catechin inhibits phosphorylation of p38 and JNK induced by oxidative stress

To further investigate the underlying mechanism by which (+)-catechin inhibits oxidative stress-induced apoptosis in fibroblasts, we determined whether oxidative stress-induced phosphorylation of JNK and p38 was inhibited by treatment with 10 μM (+)-catechin. The results clearly show that H_2O_2-induced phosphorylation of p38 and JNK was suppressed by (+)-catechin treatment (Figure 6).

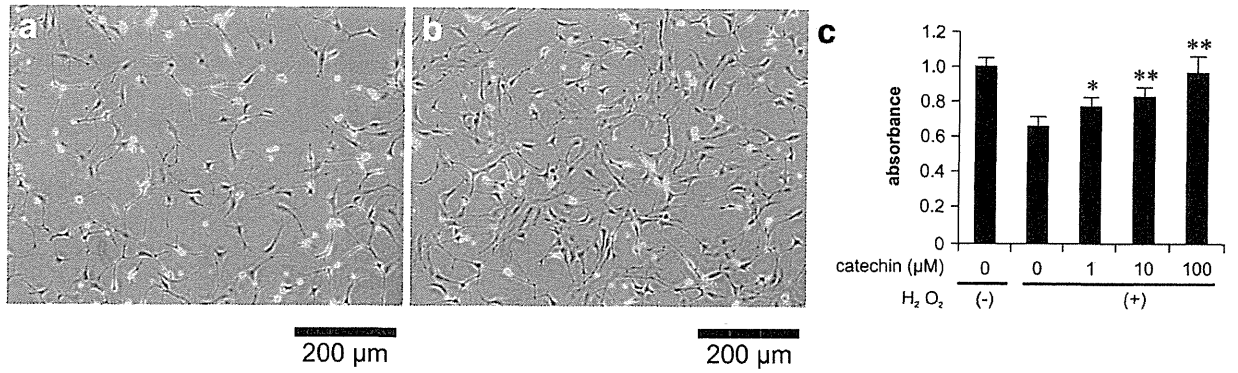

Figure 2 Inhibitory effect of (+)-catechin on oxidative stress-induced cell death in fibroblasts. After incubation with serum-free medium for 24 h, fibroblasts were treated for 30 min with (+)-catechin (0–400 μM) and then subjected to oxidative stress induction with 0.1 mM hydrogen peroxide (H_2O_2). After 24 h, cell viability was evaluated. **(a)** Representative microscopic images of cell death induced by oxidative stress **(a)** and inhibitory effect of (+)-catechin on oxidative stress-induced cell death **(b)**. Cell viability was assessed by the MTT assay **(c)**. Data are expressed as the mean ± SEM. *P < 0.05, **P < 0.01.

(+)-catechin is less cytotoxic than EGCG in fibroblasts

The MTT assay showed that fibroblasts were viable when incubated with high concentrations of (+)-catechin. In contrast, EGCG at 200 and 400 μM significantly decreased cell viability (Figure 7).

Discussion

In the present study, we demonstrate an inhibitory effect of (+)-catechin on oxidative stress-induced apoptosis in fibroblasts, accompanied by amelioration of the phosphorylation of p38 and JNK induced by oxidative stress.

We focused on fibroblasts because they participate in skin maintenance and renewal. In the skin, fibroblasts play a key role in the production of extracellular matrix components, including collagen, elastin, and hyaluronic acid. In clinical aesthetic medicine, epidermal or intradermal injection of hyaluronic acid is performed to obtain glossy and healthy skin (microinjections of hyaluronic acid, vitamins, minerals, and amino acids into the superficial layer of the skin) [15]. Other techniques, such as implanting activated fibroblasts in the skin, are also known to revive the skin to be glossy and healthy (intradermal injection of cultivated skin fibroblasts into wrinkles) [16-18]. However, these therapies are associated with a high cost and may provoke adverse events, including misplacement, allergy, nodules, necrosis, abscesses, and rejection. In contrast, the use of health supplements, such as green tea and food-derived active substances, is a safer and beneficial anti-aging method.

The integrity and functions of the skin barrier may be impaired by excessive exposure to allergens, chemicals, ultraviolet light, and dehydration. Failure of the skin barrier would subsequently lead to infections with pathogens and result in inflammatory responses. Locally produced reactive oxygen species are also known to inhibit the growth of epithelial cells and fibroblasts by inducing apoptosis and inhibiting collagen and hyaluronic acid production, all of which have been implicated in aging processes leading to skin wrinkles and sagging. Our present study suggests that (+)-catechin is a potential candidate for suppressing oxidative stress-induced apoptosis of skin fibroblasts, which may in turn reverse the reduction of fibroblast-derived

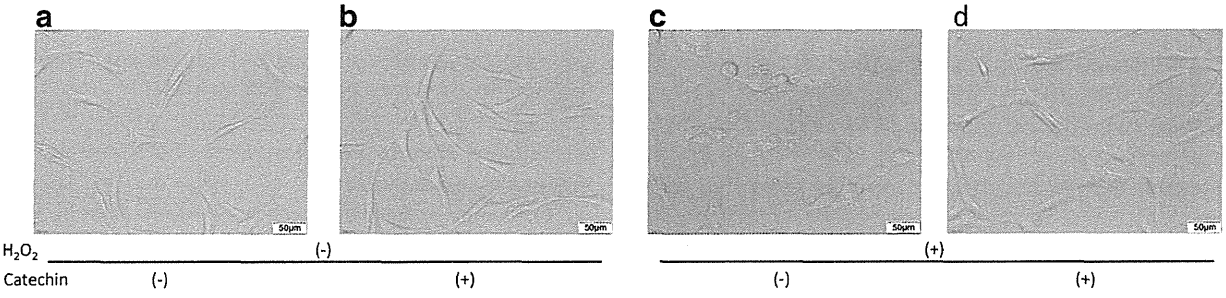

Figure 3 Microscopic images of H_2O_2-induced apoptotic cell death and inhibitory effect of (+)-catechin against H_2O_2-induced cell death. **(a)** The image of non-loading control cells. After incubation with serum-free medium for 24 h, fibroblasts were treated for 30 min with 10 μM (+)-catechin **(b)**, **(d)**. And then subjected to oxidative stress induction with 0.1 mM H_2O_2 **(c)**, **(d)**. After 24 h, microscopic morphological changes were evaluated.

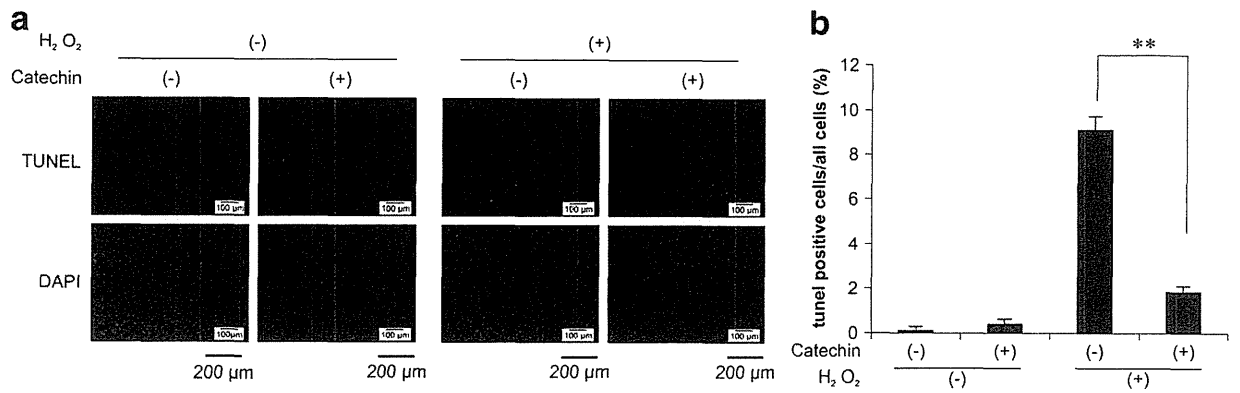

Figure 4 Inhibitory effect of (+)-catechin on oxidative stress-induced apoptosis in fibroblasts. After incubation with serum-free medium for 24 h, fibroblasts were treated for 30 min with 10 μM (+)-catechin and then subjected to oxidative stress induction with 0.1 mM hydrogen peroxide (H_2O_2). After 24 h, apoptosis was evaluated by TUNEL staining. **(a)** Microscopic findings of TUNEL staining for detection of apoptotic cells. **(b)** For evaluation of apoptosis, 100 cells were randomly selected and the percentage of TUNEL-positive cells was measured. Data are expressed as the mean ± SEM. **P < 0.01.

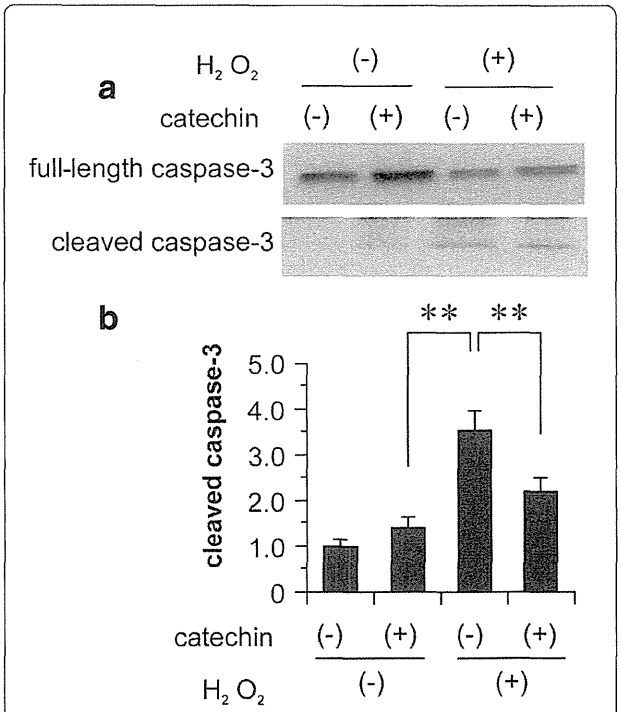

Figure 5 Effect of (+)-catechin on activation of caspase-3 by H_2O_2-induced oxidative stress in fibroblasts. After incubation with serum-free medium for 24 h, fibroblasts were treated for 30 min with 10 μM (+)-catechin and then subjected to oxidative stress induction with 0.1 mM hydrogen peroxide (H_2O_2). After 1 h, activation of caspase-3 was determined by SDS-PAGE and western blotting analysis using an anti-cleaved caspase-3 antibody. **(a)** Representative images of western blot analysis for cleaved and total caspase-3. **(b)** Expression levels of cleaved caspase-3 were normalized to those of total caspase-3. Data are expressed as the mean ± SEM. **P < 0.01.

production of collagen and hyaluronic acid. Other reports suggest that EGCG, another type of catechin, is also a potential candidate for suppressing oxidative stress-induced apoptosis of skin fibroblasts [19]; however, our present study showed that (+)-catechin is less cytotoxic than EGCG, suggesting that for therapeutic and preventive purposes (+)-catechin may be superior to EGCG.

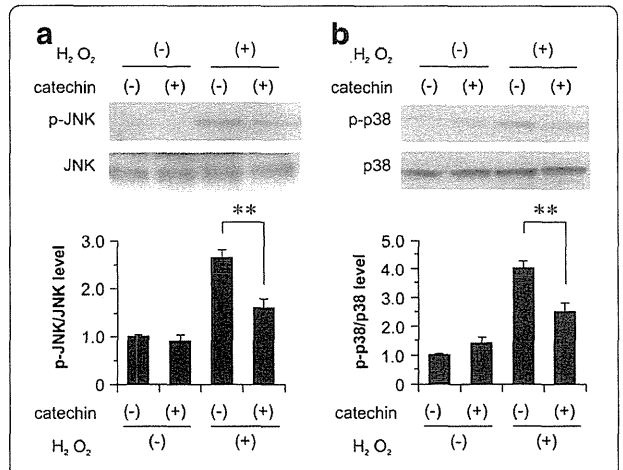

Figure 6 Inhibitory effect of (+)-catechin on phosphorylation of p38 and JNK induced by oxidative stress in fibroblasts. After incubation with serum-free medium for 24 h, fibroblasts were treated for 30 min with 10 μM (+)-catechin and then subjected to oxidative stress induction with 0.1 mM hydrogen peroxide (H_2O_2). After 1 h, cells were collected, and phosphorylation of p38 and JNK was determined by SDS-PAGE and western blotting analysis using anti-phospho p38 and anti-phospho JNK antibodies. **(a)** Results of western blotting for phosphorylation of **(a)** p38 and **(b)** JNK. Phosphorylation levels of p38 and JNK were normalized to those of total p38 and JNK, respectively. Data are expressed as the mean ± SEM. **P < 0.01.

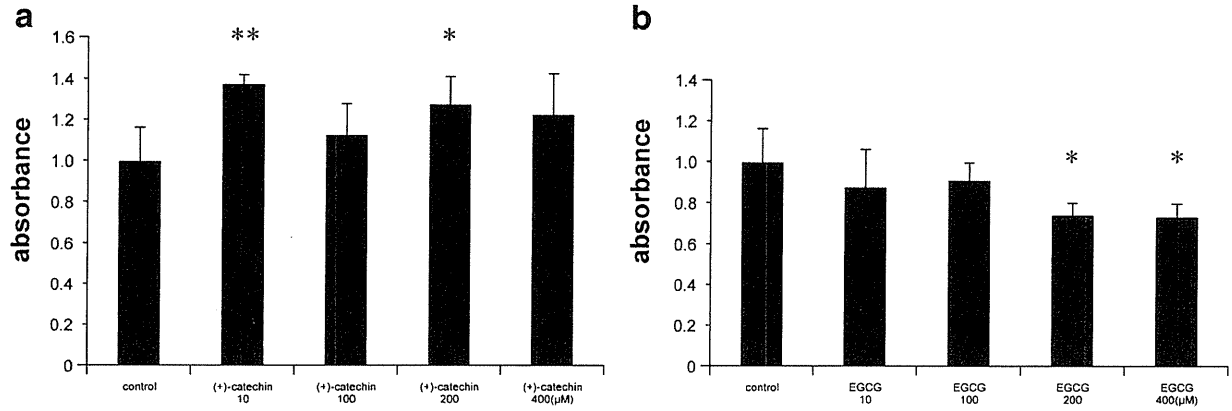

Figure 7 Comparative evaluation of cytotoxicity between (+)-catechin and EGCG in fibroblasts. Fibroblasts were treated with PBS (control) or the indicated concentrations of **(a)** (+)-catechin and **(b)** EGCG for 24 h. Cell viability was assessed by the MTT assay. Data are expressed as the mean ± SEM. *P < 0.05 and **P < 0.01.

To elucidate the underlying mechanisms by which (+)-catechin inhibits oxidative stress-induced apoptosis in fibroblasts, we focused on the effects of (+)-catechin on the phosphorylation of p38 and JNK, both of which are key molecules for oxidative stress-induced apoptosis [14]. JNK and p38 belong to the family of stress kinases and have been shown to be required for biological stress responses, such as apoptosis induced by UV, radiation, oxidative stress, heat shock, and tumor necrosis factor (TNF)-α stimulation. It has been reported that H_2O_2 signaling through TNF receptor 1 selectively activates JNK and p38 [20,21]. JNK plays an important role in controlling cell death and is known to affect the function of Bcl-2 family molecules, which suppress apoptosis. Specifically, phosphorylation of Bcl-2 by JNK results in the inhibition of Bcl-2 function and therefore induces the activation of apoptosis [20,21]. In contrast, p38 MAPK is known to be involved in the activation of apoptosis-modulating proteins, such as Fas and Bax [21]. Collectively, our present study suggests that (+)-catechin exerts anti-apoptotic effects against oxidative stress by inhibiting the phosphorylation of p38 and JNK. The precise mechanisms by which (+)-catechin suppresses the phosphorylation of JNK and p38 will be a future research topic.

Although (+)-catechin was found to exert anti-apoptotic effects in the present study, previous reports have shown both pro-apoptotic and anti-apoptotic effects of catechins. In particular, EGCG, a molecule in the same catechin group, was suggested to play a role in growth inhibition and apoptosis induction in a variety of cancer cells [22]. In contrast, EGCG was reported to have an anti-apoptotic effect in renal mesangial cells [23] and endothelial cells [24], similar to our results in the present study. Therefore, we speculate that the effect of catechins on apoptosis may vary according to cell type and the nature of pathogenesis. Given the different cell-specific responses of catechins, it is important to establish an appropriate strategy for using catechins for treatment and prevention of various diseases. It would be ideal for catechins have suppressive actions against cancers and protective effects for organs such as the kidneys and cardiovascular system. Accumulating evidence on the preventive effect of catechins and green tea against various systemic diseases, including cancers, diabetes, and hypertension, suggests little potential harm to human health from high consumption of catechins and green tea for maintenance of skin beauty.

Conclusions

(+)-Catechin exerts preventive effects against oxidative stress-induced apoptosis in fibroblasts. The underlying mechanism may involve the inhibition of p38 and JNK phosphorylation. As a safe green tea-derived antioxidant, (+)-catechin could be suitable for long-term prevention of oxidative stress-induced skin aging, considering the action of skin fibroblasts on the preservation of healthy, youthful skin.

Abbreviations

EGCG: (−)-epigallocatechin gallate; EGC: (−)-epigallocatechin; ECG: (−)-epicatechin gallate; EC: (−)-epicatechin; JNK: c-Jun terminal kinase MTT, 3-(4,5-dimethylthiazole-2-yl)-2,5-diphenyltetrazolium bromide; TdT: Terminal deoxynucleotidyl transferase; TMR: Tetramethylrhodamine; TUNEL: Terminal deoxynucleotidyl transferase (TdT)-mediated dUTP-biotin nick end labeling.

Competing interests

The authors declare that they have no competing interests.

Authors' contributions

TT designed and performed the study and wrote the manuscript. SK designed and performed the study and revised the manuscript. RY, TF, TK, KY, and KH helped to perform the study. TM, YH, KT, KM, KS, SM, and MT provided technical support. All authors read and approved the final manuscript.

Acknowledgements

This work was supported by the Mishima Kaiun Memorial Foundation. The authors are very grateful to Tetsuya Tanigawa for his advice.

Author details
[1]Department of Plastic Surgery, Osaka University Graduate School of Medicine, Suita-shi, Osaka, Japan. [2]Department of Child Development and Molecular Brain Science, United Graduate School of Child Development, Osaka University, Suita-shi, Osaka, Japan. [3]Department of Research & Development Noevir Co., Ltd. Higashiomi, Shiga, Japan. [4]Division of Molecular Brain Science, Research Institute of Traditional Asian Medicine, Kinki University, Osakasayama, Osaka, Japan. [5]Division of Plastic and Reconstructive Surgery, Niigata University Graduate School of Medicine, Niigata-shi, Niigata, Japan.

Received: 24 September 2013 Accepted: 24 March 2014
Published: 8 April 2014

References

1. Baumann L: **Skin ageing and its treatment.** *J Pathol* 2007, **211**:241–251.
2. Fenske NA, Lober CW: **Structural and functional changes of normal aging skin.** *J Am Acad Dermatol* 1986, **15**:571–585.
3. Callaghan TM, Wilhelm KP: **A review of ageing and an examination of clinical methods in the assessment of ageing skin. Part I: Cellular and molecular perspectives of skin ageing.** *Int J Cosmet Sci* 2008, **30**:313–322.
4. Rice-Evans CA, Miller NJ, Paganga G: **Structure-antioxidant activity relationships of flavonoids and phenolic acids.** *Free Radic Biol Med* 1996, **20**:933–956.
5. Valcic S, Muders A, Jacobsen NE, Liebler DC, Timmermann BN: **Antioxidant chemistry of green tea catechins. Identification of products of the reaction of (−)-epigallocatechin gallate with peroxyl radicals.** *Chem Res Toxicol* 1999, **12**:382–386.
6. Ruch RJ, Cheng SJ, Klaunig JE: **Prevention of cytotoxicity and inhibition of intercellular communication by antioxidant catechins isolated from Chinese green tea.** *Carcinogenesis* 1989, **10**:1003–1008.
7. Higdon JV, Frei B: **Tea catechins and polyphenols: health effects, metabolism, and antioxidant functions.** *Crit Rev Food Sci Nutr* 2003, **43**:89–143.
8. Cavet ME, Harrington KL, Vollmer TR, Ward KW, Zhang JZ: **Anti-inflammatory and anti-oxidative effects of the green tea polyphenol epigallocatechin gallate in human corneal epithelial cells.** *Mol Vis* 2011, **17**:533–542.
9. Steinmann J, Buer J, Pietschmann T, Steinmann E: **Anti-infective properties of epigallocatechin-3-gallate (EGCG), a component of green tea.** *Br J Pharmacol* 2013, **168**:1059–1073.
10. Sharma A, Gupta S, Sarethy IP, Dang S, Gabrani R: **Green tea extract: possible mechanism and antibacterial activity on skin pathogens.** *Food Chem* 2012, **135**:672–675.
11. Achour M, Mousli M, Alhosin M, Ibrahim A, Peluso J, Muller CD, Schini-Kerth VB, Hamiche A, Dhe-Paganon S, Bronner C: **Epigallocatechin-3-gallate up-regulates tumor suppressor gene expression via a reactive oxygen species-dependent down-regulation of UHRF1.** *Biochem Biophys Res Commun* 2013, **430**:208–212.
12. Zhang Y, Yang ND, Zhou F, Shen T, Duan T, Zhou J, Shi Y, Zhu XQ, Shen HM: **(−)-Epigallocatechin-3-gallate induces non-apoptotic cell death in human cancer cells via ROS-mediated lysosomal membrane permeabilization.** *PLoS One* 2012, **7**:e46749.
13. Fujimura Y, Sumida M, Sugihara K, Tsukamoto S, Yamada K, Tachibana H: **Green tea polyphenol EGCG sensing motif on the 67-kDa laminin receptor.** *PLoS One* 2012, **7**:e37942.
14. Naderi J, Hung M, Pandey S: **Oxidative stress-induced apoptosis in dividing fibroblast involves activation of p38 MAP kinase and over-expression of Bax: resistance of quiescent cells to oxidative stress.** *Apoptosis* 2003, **8**:91–100.
15. Alster TS, West TB: **Human-derived and new synthetic injectable materials for soft-tissue augmentation: current status and role in cosmetic surgery.** *Plast Reconstr Surg* 2000, **105**:2515–2525.
16. Eça LP, Pinto DG, de Pinho AM, Mazzetti MP, Odo ME: **Autologous fibroblast culture in the repair of aging skin.** *Dermatol Surg* 2012, **38**:180–184.
17. Jäger C, Brenner C, Habicht J, Wallich R: **Bioactive reagents used in mesotherapy for skin rejuvenation *in vivo* induce diverse physiological processes in human skin fibroblasts *in vitro*- a pilot study.** *Exp Dermatol* 2012, **21**:72–75.
18. Solakoglu S, Tiryaki T, Ciloglu SE: **The effect of cultured autologous fibroblasts on longevity of cross-linked hyaluronic acid used as a filler.** *Aesthet Surg J* 2008, **28**:412–416.
19. Feng B, Fang Y, Wei SM: **Effect and mechanism of epigallocatechin-3-gallate (EGCG). against the hydrogen peroxide-induced oxidative damage in human dermal fibroblasts.** *J Cosmet Sci* 2013, **64**:35–44.
20. Liu J, Lin A: **Role of JNK activation in apoptosis: a double-edged sword.** *Cell Res* 2005, **15**:36–42.
21. Wada T, Penninger JM: **Mitogen-activated protein kinases in apoptosis regulation.** *Oncogene* 2004, **23**:2838–2849.
22. Yang CS, Wang X, Lu G, Picinich SC: **Cancer prevention by tea: animal studies, molecular mechanisms and human relevance.** *Nat Rev Cancer* 2009, **9**:429–439.
23. Liang YJ, Jian JH, Liu YC, Juang SJ, Shyu KG, Lai LP, Wang BW, Leu JG: **Advanced glycation end products-induced apoptosis attenuated by PPARδ activation and epigallocatechin gallate through NF-κB pathway in human embryonic kidney cells and human mesangial cells.** *Diabetes Metab Res Rev* 2010, **26**:406–416.
24. Choi YJ, Jeong YJ, Lee YJ, Kwon HM, Kang YH: **(−)Epigallocatechin gallate and quercetin enhance survival signaling in response to oxidant-induced human endothelial apoptosis.** *J Nutr* 2005, **135**:707–713.

doi:10.1186/1472-6882-14-133
Cite this article as: Tanigawa *et al.*: (+)-Catechin protects dermal fibroblasts against oxidative stress-induced apoptosis. *BMC Complementary and Alternative Medicine* 2014 **14**:133.

L-Arginine Stimulates Fibroblast Proliferation through the GPRC6A-ERK1/2 and PI3K/Akt Pathway

Takashi Fujiwara[1], Shigeyuki Kanazawa[1]*, Ryoko Ichibori[1], Tomoko Tanigawa[1], Takuya Magome[2], Kenta Shingaki[3], Shingo Miyata[4], Masaya Tohyama[4], Ko Hosokawa[1]

1 Department of Plastic Surgery, Osaka University Graduate School of Medicine, Suita-shi, Osaka, Japan, **2** Department of Child Development and Molecular Brain Science, United Graduate School of Child Development, Osaka University, Suita-shi, Osaka, Japan, **3** Department of Research & Development Noevir Co., Ltd. Higashiomi, Shiga, Japan, **4** Division of Molecular Brain Science, Research Institute of Traditional Asian Medicine, Kinki University, Osakasayama, Osaka, Japan

Abstract

L-Arginine is considered a conditionally essential amino acid and has been shown to enhance wound healing. However, the molecular mechanisms through which arginine stimulates cutaneous wound repair remain unknown. Here, we evaluated the effects of arginine supplementation on fibroblast proliferation, which is a key process required for new tissue formation. We also sought to elucidate the signaling pathways involved in mediating the effects of arginine on fibroblasts by evaluation of extracellular signal-related kinase (ERK) 1/2 activation, which is important for cell growth, survival, and differentiation. Our data demonstrated that addition of 6 mM arginine significantly enhanced fibroblast proliferation, while arginine deprivation increased apoptosis, as observed by enhanced DNA fragmentation. In vitro kinase assays demonstrated that arginine supplementation activated ERK1/2, Akt, PKA and its downstream target, cAMP response element binding protein (CREB). Moreover, knockdown of GPRC6A using siRNA blocked fibroblast proliferation and decreased phosphorylation of ERK1/2, Akt and CREB. The present experiments demonstrated a critical role for the GPRC6A-ERK1/2 and PI3K/Akt signaling pathway in arginine-mediated fibroblast survival. Our findings provide novel mechanistic insights into the positive effects of arginine on wound healing.

Citation: Fujiwara T, Kanazawa S, Ichibori R, Tanigawa T, Magome T, et al. (2014) L-Arginine Stimulates Fibroblast Proliferation through the GPRC6A-ERK1/2 and PI3K/Akt Pathway. PLoS ONE 9(3): e92168. doi:10.1371/journal.pone.0092168

Editor: Ichiro Aoki, Yokohama City University School of Medicine, Japan

Received July 9, 2013; **Accepted** February 19, 2014; **Published** March 20, 2014

Funding: The authors have no support or funding to report.

Competing Interests: The authors have the following interests: Kenta Shingaki is employed by Noevir Co., Ltd. There are no patents, products in development or marketed products to declare. This does not alter the authors' adherence to all the PLOS ONE policies on sharing data and materials, as detailed online in the guide for authors.

* E-mail: kanazawa@psurg.med.osaka-u.ac.jp

Introduction

L-Arginine, traditionally classified as a nonessential amino acid, is now considered conditionally essential for tissue healing and survival [1,2]. In normal conditions, L-arginine is produced endogenously according to the needs of the tissues/cells; however, endogenous synthesis of L-arginine may be insufficient during metabolic stress, organ maturation, and development [3]. A number of studies have demonstrated that arginine supplementation is also important in wound healing. The beneficial effects of L-arginine on wound healing are mediated by nitric oxide (NO), which is synthesized from L-arginine through the action of nitric oxide synthase during the wound healing process. In fibroblasts, NO supports collagen synthesis, which is essential for scar formation [4,5]. However, little is known about the molecular mechanisms mediating this process. Moreover, while L-arginine has been shown to stimulate proliferation in intestinal cells and trophectoderm cells [6,7], the effects of L-arginine treatment on fibroblast proliferation have not been reported.

Wound healing involves a cascade of events, including blood clotting, inflammation, new tissue formation, and tissue remodeling [8]. This complex process requires the collaborative efforts of many types of cells: immune cells, endothelial cells, keratinocytes, and fibroblasts [9]. Fibroblast migration and proliferation within the wound site play a key role in the formation of granulation tissue. Fibroblasts migrate into the wound tissue, where they proliferate and deposit extracellular matrix. Various intracellular and intercellular pathways are activated and coordinated to facilitate these processes of fibroblast migration and proliferation [10–12]. L-arginine has been shown to enhance cell migration via the phosphoinositol 3-kinase/mammalian target of rapamycin pathway in enterocytes [13]. Moreover, a number of mammalian target of rapamycin pathway kinases interact with the actin cytoskeleton in advancing lamellipodia and regulate fibroblast migration [14]. However, the effects of L-arginine supplementation on fibroblast proliferation have not been clearly elucidated.

Members of the mitogen-activated protein kinase (MAPK) family represent important mediators of signal transduction pathways and are required to facilitate the effects of growth factors and other proteins. The pathway mediated by Ras-dependent extracellular signal-regulated kinase (ERK) 1/2, the prototypical MAPK, is one of the most frequently studied signaling systems; ERK1/2 signaling is known to control the expression of various cell-cycle regulators and to participate in multiple cellular functions, such as proliferation, differentiation, and apoptosis [15–17].

Recently some studies implicated that the serine threonine kinase Akt/PKB blocks cellular apoptosis and promote cell survival in response to growth factor induction [18,19]. Further-

more, PI3K and MAPK activation by basic amino acids such as L-lysine, L-arginine and L-ornithine is known be activated by GPRC6A which is a member of the G protein-coupled receptor 3 family. However, the signaling pathway of fibroblast cellular function by L-arginine through activation of GPRC6A receptor is not well elucidated [20,21].

In the present study, we investigated the effects of L-arginine on fibroblast proliferation and examined the involvement of the GPRC6A, Akt, ERK1/2 pathway and its downstream target, cAMP response element binding protein (CREB), in fibroblast proliferation and survival.

Results

L-Arginine Stimulated Fibroblast Proliferation

L-Arginine has been shown to stimulate the proliferation of intestinal cells and trophectoderm cells [6,7]; however, the effects of L-arginine treatment on fibroblast proliferation have not been reported. Therefore, we first examined whether treatment with L-arginine affected fibroblast proliferation (Fig. 1A, B, C). Following 24 h of L-arginine starvation, NIH3T3 and primary human dermal fibroblasts (HDF) were treated with various concentrations of L-arginine (0–7 mM) for 24 h, and cell viability was then assessed. Significant dose-dependent proliferation was observed at L-arginine concentrations above 2 mM with NIH3T3 and 4 mM with HDF. Six millimolar L-arginine produced maximum stimulation of proliferation, inducing a 3.0-fold increase in NIH3T3 fibroblast proliferation and 1.8-fold increase in HDF compared to cells deprived of L-arginine. In order to evaluate cell growth and survival of NIH3T3 and HDF with or without L-arginine treatment, we performed trypan-blue dye exclusion cell counting at 0, 6, 12, and 24 h post culture. The results demonstrated trypan-blue excluded cell increase at 12, 24 h in the group with L-arginine cultured NIH3T3 and HDF without decreasing the trypan-blue positive cells (Fig. 1C). Thus, these data demonstrated that L-Arginine induced fibroblast proliferation.

L-Arginine Decreased Apoptosis in Fibroblasts

Normal cells require growth factors for proliferation and survival. Growth factor deprivation can lead to apoptosis [22]. Therefore, we next determined whether L-arginine played an important role in preventing apoptosis by examining DNA fragmentation as a marker of apoptosis in the presence or absence of arginine (Fig. 2A, B). L-Arginine-deprived NIH3T3 and HDF demonstrated a significant increase in the percentage of terminal deoxynucleotidyltransferase-mediated dUTP-biotin nick end labeling (TUNEL)-positive cells compared with cells maintained in 6 mM arginine (NIH3T3; 10.7% ±2.9% vs. 1.3% ±0.8%, HDF; 11.1% ±2.1% vs. 1.6% ±0.9% respectively). Furthermore, we performed trypan-blue dye at 0, 6, 12, and 24 h after L-arginine treatment. After the treatment, NH3T3 and HDF both demonstrated significant decrease in trypan-bule positive cells (NIH3T3; 11.4% ±1.5% vs. 2.6% ±1.0%, HDF; 12.6% ±1.7% vs. 2.6% ±1.1% respectively at 24 h) (Fig. 2C) Thus, our data demonstrated that L-arginine decreased apoptosis in fibroblasts. In conclusion, the results suggest that L-arginine inhibits apoptosis.

L-Arginine Activated ERK1/2, PI3K-Akt, cAMP-PKA and CREB

To examine the molecular mechanisms responsible for the proliferative effects of L-arginine in fibroblasts, we evaluated arginine-dependent activation of the ERK1/2, PI3K/Akt and cAMP-PKA pathway, which plays a major role in regulating cell growth, survival, and differentiation. HDF were deprived of L-arginine for 24 h and then supplemented with 6 mM L-arginine for different times (0–30 min). We found that L-arginine supplementation significantly increased levels of phosphorylated ERK1/2, Akt and PKA at 5–15 min (Fig. 3A, B and C).

Since phosphorylated ERK1/2 is known to phosphorylate transcription factors, such as CREB, which regulates the transcription of genes involved in cellular metabolism, growth, migration, and proliferation, we next examined the effects of arginine on CREB phosphorylation. Similar to the effects observed for ERK1/2, CREB phosphorylation was also significantly increased at 5, 15, and 30 min with L-arginine (2.4, 2.3, and 3.8-fold increases, respectively, compared to cells deprived of arginine; Fig. 3D). To confirm the involvement of ERK1/2 in L-arginine induced CREB phosphorylation, we inhibited ERK1/2 by U-0126, a selective MEK inhibitor. The results showed that L-arginine-induced CREB phosphorylation significantly decreased by 68% with ERK1/2 inhibition (Fig. 3E). Taken together, these data showed that L-arginine activated both ERK1/2 and its downstream effector, CREB.

L-Arginine-induced Fibroblast Proliferation was Blocked by GPRC6A Knockdown

Since GPRC6A is known to be a receptor for amino acids for basic amino acids such as L-lysine, L-arginine and L-ornithine, we speculated that GPRC6A would be stimulated by L-arginine to activate ERK1/2, Akt, PKA, and CREB. Therefore, we used siRNA to knockdown GPRC6A in HDF to investigate the activation of ERK1/2, Akt, PKA, and CREB. As a result, activation of ERK1/2, Akt, PKA, and CREB were all inhibited due to the knockdown of GPRC6A (69%, 64%, 67%, 74% respectively)(Fig. 4 A, B, C and D). In conclusion, we believe that GPRC6A resides in the upper stream of ERK1/2, Akt, PKA, and CREB to function as the receptor of L-arginine to regulate the cellular signaling.

In order to confirm the involvement of GPRC6A, ERK1/2, PI3K-Akt, c-AMP-PKA, and CREB activation in cellular proliferation by L-arginine, we examined the L-arginine-induced fibroblast proliferation by MTS assay using its inhibitors (U-0126, LY294002, H-89 respectively) and siRNA GPRC6A or CREB. The results demonstrated significant cell death or low cell count due to the inhibition of GPRC6A, ERK1/2, PI3K-AKT, and CREB (65%, 70%, 77%, 70% respectively) (Fig. 5). On the other hand, inhibition of PKA did not block L-arginine-induced fibroblast proliferation.

Thus, our data demonstrated that inhibition of GPRC6A, ERK1/2, Akt and CREB blocked L-arginine-induced fibroblast proliferation, thereby suggesting that L-arginine stimulated fibroblast proliferation via GPRC6A, ERK1/2 and PI3K/Akt signaling pathway.

Discussion

Supplemental L-arginine has been shown to improve wound healing, as manifested by enhanced T-cell-mediated immune function [23,24], increased wound breaking strength, and collagen deposition [2,25]. Arginine treatment has also been shown to regulate the cytokine environment at the wound site, reducing tissue interleukin-6 levels in the wound [26]. Thus, L-arginine decreases the adverse effects of increased inflammation in the wound. However, despite the great number of studies demonstrating the beneficial effects of arginine on wound healing, the molecular mechanisms through which it mediates these effects have not been well investigated. Moreover, the effects of L-arginine

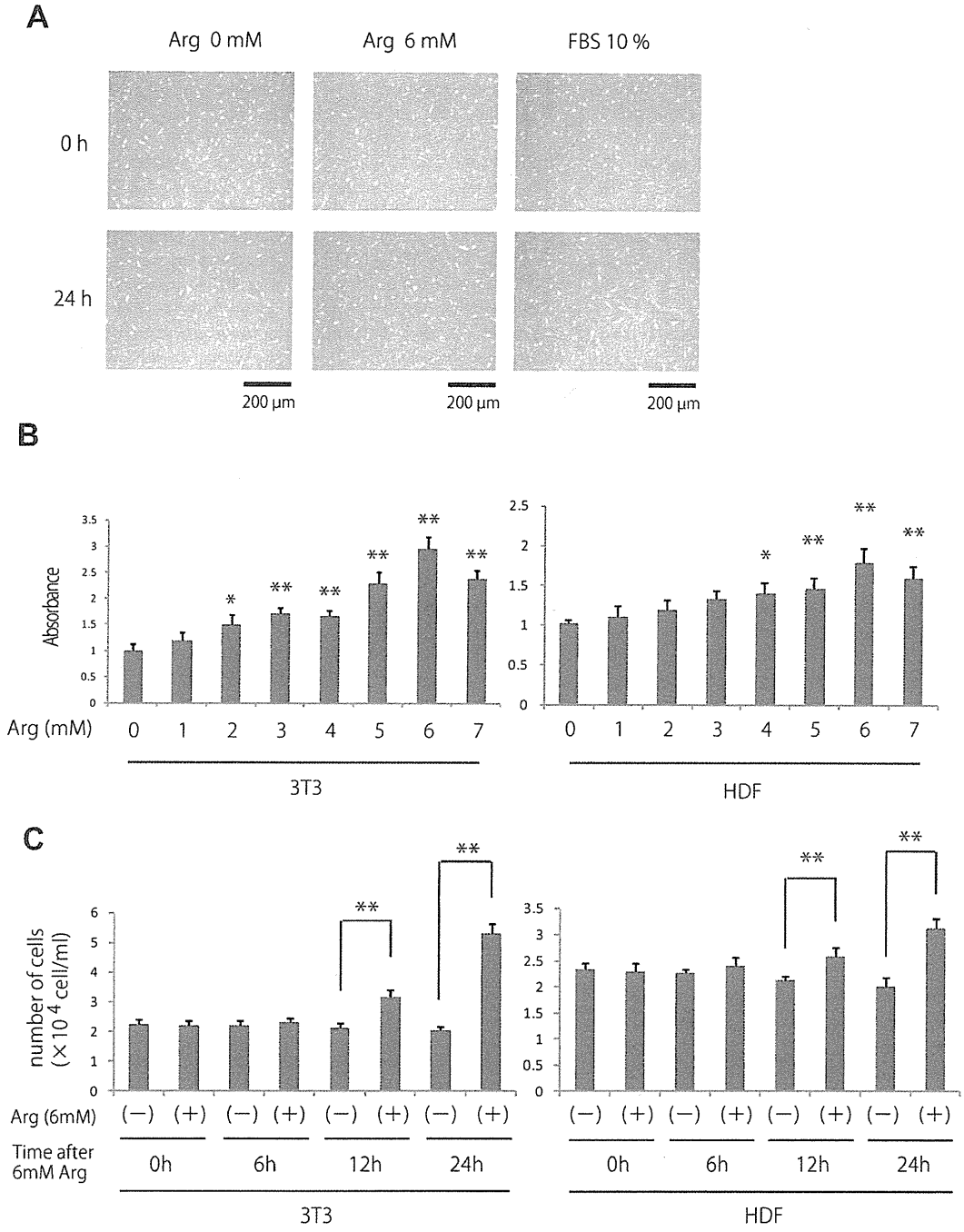

Figure 1. Effects of L-arginine on fibroblast proliferation. (A) This photograph shows human dermal fibroblast at 24 h after treatment with or without 6 mM L-arginine. DMEM with 10%FBS was used as positive control. (B) Fibroblast proliferation was determined by MTS assay after treatment with the indicated concentrations of L-arginine (0–7 mM). Results are expressed as the mean ± SEM of 3 independent experiments. *$p<0.05$, **$p<0.01$, as compared with the control group (Student's t test). (C) The number of trypan blue negative fibroblast at 0, 6, 12 and 24 h after treated with 0 or 6 mM L-arginine. **$p<0.01$, as compared with the control group (Student's t test).
doi:10.1371/journal.pone.0092168.g001

on fibroblasts, important cells in the wound healing process that are responsible for collagen synthesis in granulation tissue have not been clearly elucidated.

In our present study, we demonstrated that L-arginine supplementation stimulates fibroblast proliferation and that deprivation of L-arginine facilitates fibroblast apoptosis, suggesting that arginine possesses fibroblast proliferation promoting and anti-apoptotic effects. Consistent with this, arginine has been shown to induce proliferation in endothelial cells, intestinal cells and trophectoderm cells [6,7]. Although we did not show the in vivo role of L-arginine in wound healing, we believe that our data can support the idea of L-arginine taking a great part in wound healing

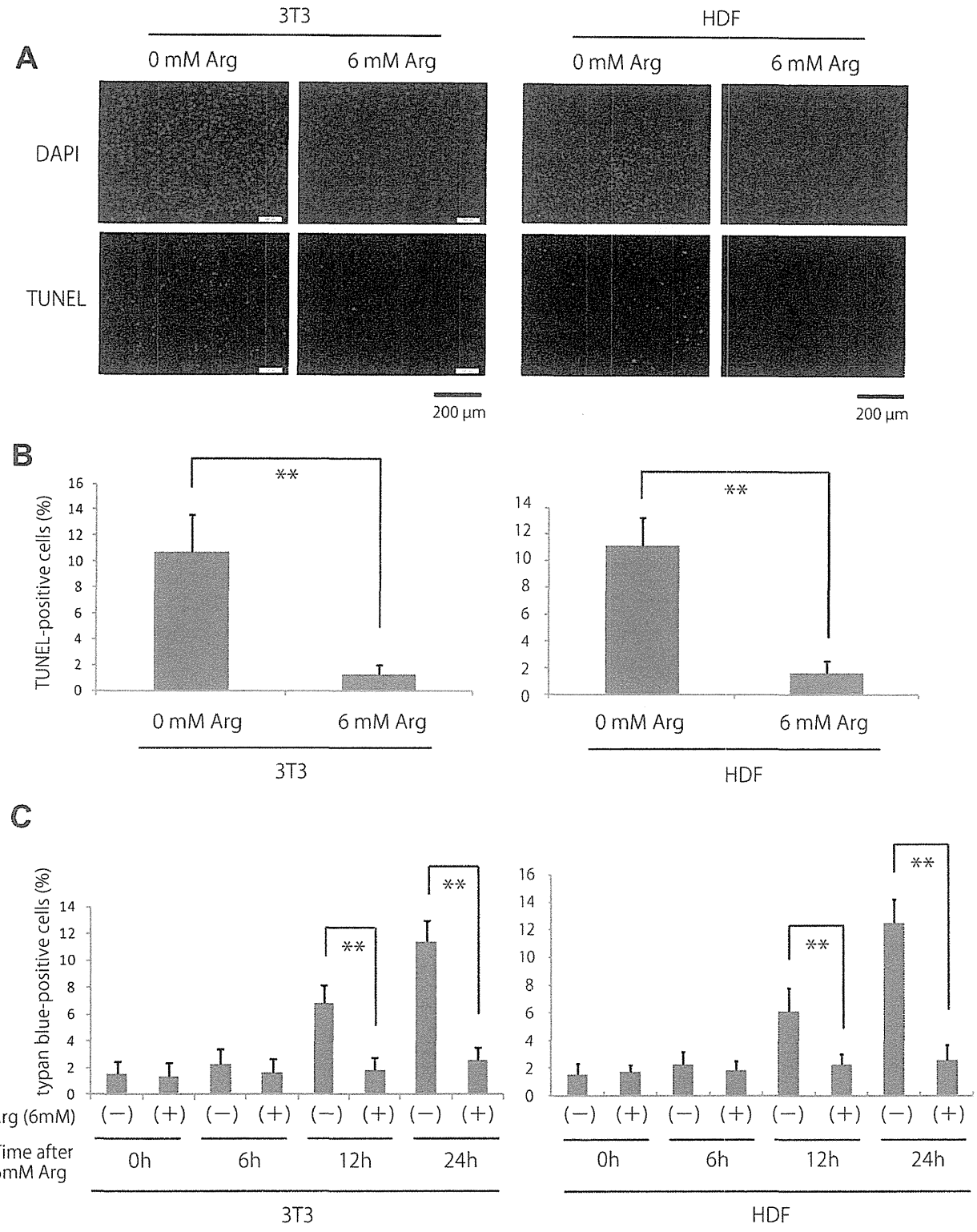

Figure 2. Effects of L-arginine deprivation and stimulation on apoptosis in fibroblasts. (A) Apoptosis was measured using the TUNEL assay in L-arginine-deprived and -treated fibroblasts. (B) Quantification of the data from (A). $^{**}p<0.01$, as compared with the control group (Student's t test). (C) The number of cell death using the 0.1% trypan blue staining in L-arginine-deprived and -treated fibroblasts. $^{**}p<0.01$, as compared with the control group (Student's t test).
doi:10.1371/journal.pone.0092168.g002

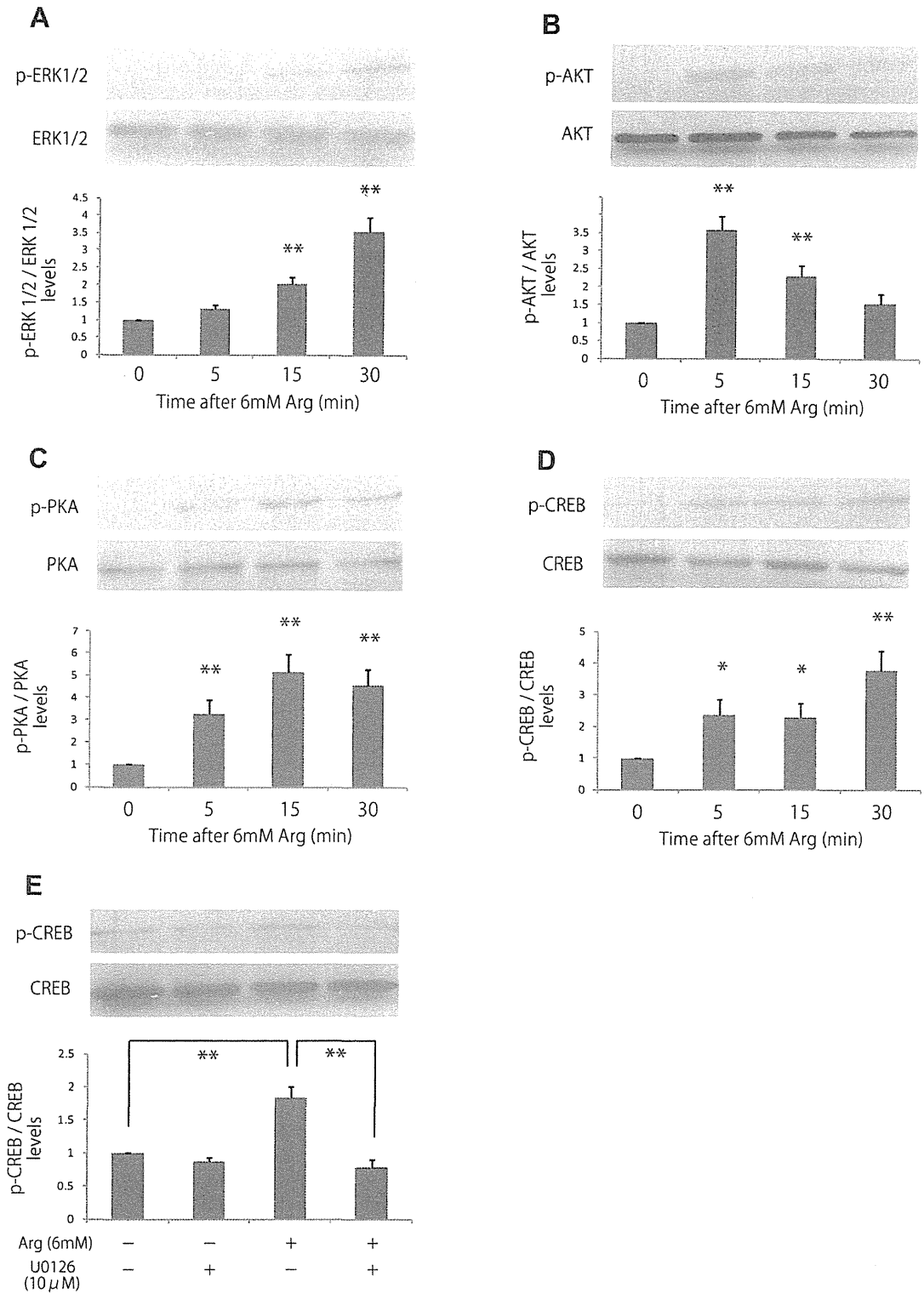

Figure 3. Effects of L-arginine stimulation on the activities of ERK, Akt, PKA and CREB. (A, B, C, D) ERK, Akt, PKA and CREB activities were analyzed by immunoblotting at 5, 15, and 30 min after stimulation with 6 mM L-arginine. Densitometry measurements for p-ERK, p-Akt, p-PKA and p-CREB were normalized to the amount of total ERK, Akt, PKA and CREB, respectively. (E) Fibroblasts were treated with 10 μM U0126, and then cells were stimulated with 6 mM L-arginine. The activities of CREB were analyzed by immunoblotting. Results are presented as the fold change compared with untreated cells. Data are expressed as the mean ± SEM of 3 independent experiments (*$p<0.05$, **$p<0.01$, Tukey's post hoc test).
doi:10.1371/journal.pone.0092168.g003

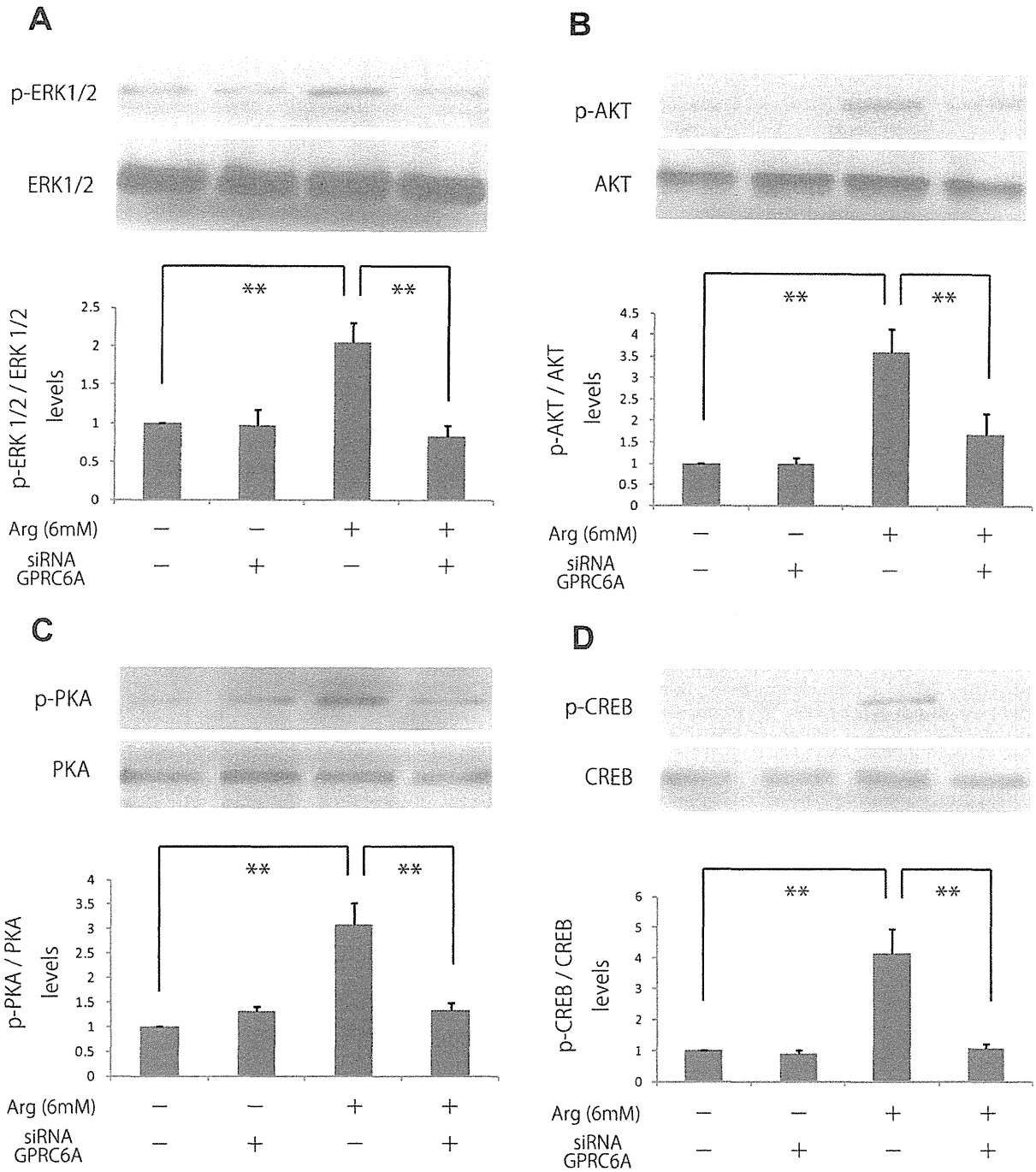

Figure 4. Effects of knockdown of GPRC6A on the activities of ERK, Akt, PKA and CREB in L-arginine-treated fibroblasts. (A, B, C, D) Fibroblasts were treated with si RNA GPRC6A and then cells were stimulated with 6 mM L-arginine. The activities of ERK, Akt, PKA and CREB were analyzed by immunoblotting. Densitometry measurements for p-ERK, p-Akt, p-PKA and p-CREB were normalized to the amount of total ERK, Akt, PKA, and CREB, respectively. Results are presented as the fold change compared with the control group. Data are expressed as the mean ± SEM of 3 independent experiments (**$p<0.01$, Tukey's post hoc test).
doi:10.1371/journal.pone.0092168.g004

by promoting fibroblast cellular function. To support our findings, Yatabe et al demonstrated the efficacy of clinical application of L-arginine as ARGINAID WATER for accelerating wound healing in pressure ulcer patients [27]. Since the concentration of L-arginine used for our study is much higher compare to clinical use, we assume that L-arginine can function with much lower concentration in vivo. For future study, we plan to investigate the in vivo function of L-arginine in murine or human individuals.

MAPK signaling plays an important role in complex cellular processes, such as proliferation, differentiation, development,

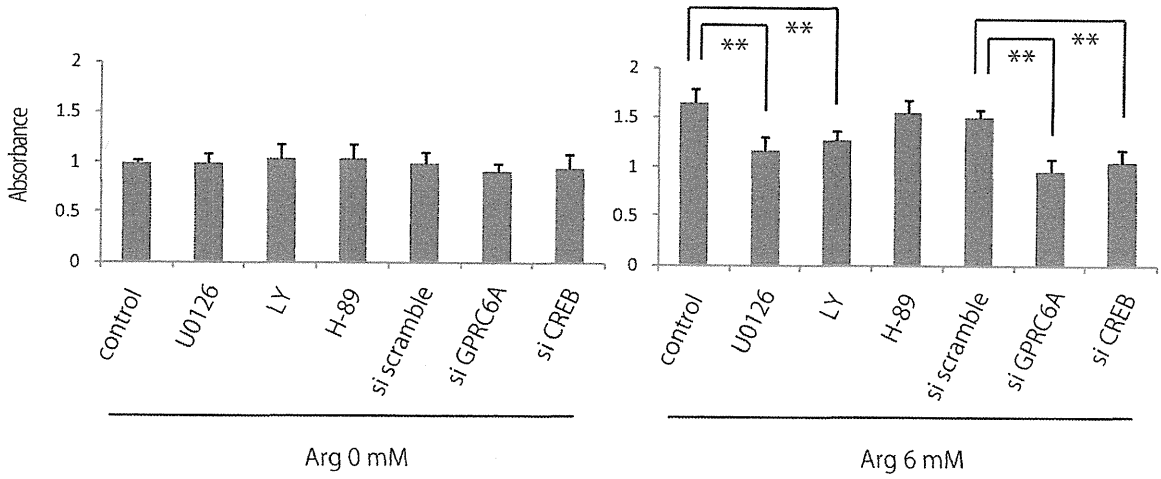

Figure 5. Effects of inhibition of ERK, Akt, PKA, CREB and GPRC6A on the proliferation of L-arginine-treated fibroblasts. Fibroblast proliferation was measured by MTS assay after pretreatment with 0 or 6 mM L-arginine and subsequent treatment with 10 μM U0126, LY294002, H-89, siRNA CREB and siRNA GPRC6A. Results are expressed as the mean ± SEM of 3 independent experiments.
doi:10.1371/journal.pone.0092168.g005

transformation, and apoptosis. At least 3 MAPK families have been characterized: ERK, Jun kinase, and p38 MAPK. MAPKs, particularly ERK1/2, play an important role in proliferation, differentiation, and survival processes [15–17]. Phosphorylation of ERK1/2 has been linked to activation of CREB [28,29]; phosphorylated ERK1/2 translocates to the nucleus where it phosphorylates CREB, a transcription factor, which activates genes involved in cell proliferation. In the present study, we demonstrated that L-arginine treatment following a period of starvation resulted in the activation of ERK1/2 and CREB, suggesting the involvement of the entire ERK1/2 pathway in the response to L-arginine in human dermal fibroblasts.

Furthermore, PI3K-Akt is also an important signaling factor for cell survival other than MAPK signaling. At the same time, serine threonine kinase Akt/PKB also acts as an important mediator of metabolic factors and promotes cell survival against several apoptotic stimuli [30]. In our study, we were able to demonstrate that L-arginine induces the activation of Akt signaling and promotes fibroblast proliferation and cell survival. We supported these findings and proved that Akt is an important factor for L-arginine-induced fibroblast cell activity by showing that the activity of L-arginine is inhibited after Akt signaling inhibition.

Moreover, we investigated whether L-arginine stimulates GPRC6A which is known to be the receptor for amino acids such as L-lysine, L-arginine, L-ornithine to activate the ERK and Akt signaling pathway. We were able to prove that GPRC6A is greatly involved in activation of ERK1/2, Akt, PKA, and CREB factors with L-arginine stimulus by showing that GPRC6A knockdown inhibits ERK1/2, Akt, PKA, and CREB activation. In addition, we demonstrated that L-arginine-induced fibroblast proliferation significantly decreases with inhibition of GPRC6A, CREB, ERK1/2 and Akt but was not affected with inhibition of PKA. Therefore, we believe that PKA is not strongly involved in the activation of fibroblast proliferation. All to together, our findings suggest that fibroblast cell proliferation and anti-apoptotic effect is stimulated by L-arginine through the activation of GPRC6A, ERK1/2-CREB and PI3K/Akt pathway.

The effects of arginine supplementation may be mediated by NO synthesis. L-Arginine has been identified as a substrate for the production of the biologic effector molecule NO by a group of isoenzymes termed nitric oxygen synthases. This pathway is present in many tissues and cells, including fibroblasts. NO is a highly diffusible intercellular signaling molecule that regulates the activity of several transcription factors. NO has been shown to increase proliferation in BALB/c 3T3 fibroblasts and endothelial cells [31,32]. Studies have also identified G proteins, and particularly $p21^{ras}$, as central targets of NO [33,34]. The mechanism of $p21^{ras}$ activation is due to S-nitrosylation of a cysteine residue, which promotes guanine nucleotide exchange [34]. In addition, NO has been shown to signal downstream of $p21^{ras}$ by activation of the ERK pathway in human T cells [35]. This ERK pathway is typically activated by growth factors via a $p21^{ras}$-dependent signal transduction pathway [36,37]. Therefore, it is possible that L-arginine-induced fibroblast proliferation and ERK1/2 activation may be attributed to the synthesis of NO by nitric oxygen synthase.

In conclusion, the present experiments demonstrated a critical role for activation of GPRC6A along with the activation of ERK1/2-CREB and PI3K/Akt pathway in L-arginine-mediated fibroblast proliferation and survival. Our findings provide novel mechanistic insights into the positive effects of L-arginine on fibroblast proliferation and survival.

Materials and Methods

Cell Culture

Human dermal fibroblast and NIH 3T3 fibroblasts were used for experiments. Cells were cultured in Dulbecco's modified Eagle medium (DMEM) containing 10% fetal bovine serum, 100 U/mL penicillin, and 100 μg/mL streptomycin in a humidified incubator at 37°C with a 5% CO_2 atmosphere. L-Arginine starvation was performed by preparing L-arginine free medium using SILAC™ D-MEM (without L-arginine, L-glutamine, L-lysine) added 584 mg/L L-glutamine and 146 mg/l L-lysine. All experiments were performed in triplicate.

Cell Viability Assay

Cell survival was determined using a CellTiter 96 AQueous One Solution Cell Proliferation Assay (Promega, WI, USA). Fibroblasts were plated at a density of 5000 cells per well in 96-

well plates and incubated for 24 h in DMEM containing 10% fetal bovine serum. After L-arginine starvation for 24 h, fibroblasts were treated with ERK, Akt, PKA inhibitor (10 μM U-0126, 10 μM LY294002, 10 μM H-89) for 1 h and then treated with various concentrations of L-arginine (0–7 mM or 6 mM) for 24 h. After L-arginine treatment, 20 μL of One Solution Reagent was added into each well of the 96-well assay plate containing the samples in 100 μL of culture medium. The fibroblasts were incubated for an additional 2 h at 37°C in a humidified, 5% CO_2 atmosphere. The production of formazan produced by viable cells was measured at an absorbance of 490 nm using a 96-well plate reader.

Cell Counting with Trypan Blue Dye Exclusion

Fibroblasts were plated on 35 mm dish and incubated for 24 h in DMEM containing 10% FBS. After L-arginine starvation for 24 h the cells were treated with 0 or 6 mM L-arginine. The cells were detached by trypsinization at 0, 6, 12 and 24 h after L-arginine treatment and exposed to 0.1% trypan blue. The number of trypan blue negative cells was counted using a microscopic counting chamber.

Western Blot Analysis and Immunoprecipitation

Cultured fibroblasts were starved for 24 h in serum-free DMEM without L-arginine. Six millimolar L-arginine was then added, and cells were harvested at specified times (0–30 min). For inhibitor studies, cells were deprived of L-arginine for 24 h and then treated with MEK inhibitor (U-0126 [10 μM]) in the presence or absence of L-arginine. After treatment, cells were lysed in RIPA buffer containing 1 mM Na_3VO_4, 1 mM NaF, and Protease Inhibitor Cocktail (Roche Diagnostics, Basel, Switzerland), incubated for 20 min at 4°C, and centrifuged at 15,000×*g* for 15 min at 4°C. The proteins were separated by SDS-PAGE and electrotransferred onto Immobilon-P Transfer Membranes (Millipore Japan, Tokyo, Japan). The membranes were incubated in TBS containing 5% skim milk and 0.05% Tween-20 for 60 min and blotted with primary antibodies at 4°C overnight. The following primary antibodies were used: anti-phospho-ERK1/2 (1:1000, Cell Signaling Technology, MA, USA), anti-ERK1/2 (1:1000, Cell Signaling Technology), anti-phospho-CREB (1:1000, Cell Signaling Technology), anti-CREB (1:1000, Cell Signaling Technology), anti-phospho-Akt (1:1000, Cell Signaling Technology), anti-Akt(1:1000, Cell Signaling Technology), anti-phospho-PKA (1:1000, Cell Signaling Technology), and anti-PKA (1:1000, Cell Signaling Technology). The membranes were incubated for 1 h with anti-mouse or anti-rabbit horseradish peroxidase-linked secondary antibodies (1:2000, Cell Signaling Technology). Reaction products were visualized by detection of chemiluminescence using an ECL Western Blotting Detection System (GE Healthcare, Piscataway, NJ, USA). Quantification of relative band densities was performed by scanning densitometry using Image J software (National Institute of Health, Bethesda, MD, USA).

TUNEL Apoptosis Assay

Apoptosis was determined by TUNEL assay using an In Situ Cell Death Detection Kit TMR Red (Roche), according to the manufacturer's instructions. The fibroblasts were maintained in DMEM containing 10% fetal bovine serum for 2 days and cultured in serum-free DMEM without L-arginine for 24 h. Then, the cells treated with or without 6 mM L-arginine for 24 h. The cells were fixed with paraformaldehyde solution (4% in phosphate-buffered saline [pH 7.4]) for 60 min at room temperature and washed with PBS 5 times. Permeabilization was carried out with 0.1% Triton X-100 in PBS for 10 min, followed by incubation in a TUNEL reaction mixture containing terminal deoxynucleotidyl-transferase and TMR red-labeled nucleotides for 1 h. The coverslips were mounted onto the slides using VECTASHIELD Mounting Medium with DAPI (Vector Laboratories, Peterborough, England). Fluorescence images were taken using a microscope (model IX-70; Olympus) equipped with a CCD Camera (CoolSNAP HQ; Nippon Roper, Chiba, Japan). One hundred cells per experiment were randomly selected, and the percentage of TUNEL-positive cells was measured.

RNA Interference Experiments

siRNA duplex for the GPRC6A or CREB gene was synthesized by Invitrogen with help of the D-LUX Designer (Invitrogen Japan, Tokyo, Japan). The GPRC6A siRNA (59-GGGAUGCU-GAUUUACUUCAUAGCUU-39) was designed to target coding the region of human GPRC6A mRNA sequence (GenBank accession no. NM_148963). The CREB1 siRNA (59-GCCCAG-CAACCAAGUUGUUGUUCAA-39) was designed to target coding the region of human CREB1 mRNA sequence (GenBank accession no. NM_004379). Primary human fibroblasts were transfected with GPRC6A or CREB1 siRNA using Lipofectamine RNAiMAX (Invitrogen Japan) and Opti-MEM (Invitrogen Japan) by the manufacturer's protocol. The final concentration of siRNA was 10 nM. Stealth RNAi Negative Control Medium GC Duplex (Invitrogen Japan) was used as a control. The transfected cells were used for experiments after 48 h.

Statistical Analysis

All data shown are expressed as the mean ± SE of the values obtained from 3 individual experiments. Data from each independent experiment were normalized to the control sample in that particular experiment. Differences between results were analyzed by using Student's t test. Multiple group comparisons were performed using a one-way analysis of variance, followed by the Tukey's post hoc test. *P*-values of less than 0.05 were considered statistically significant.

Author Contributions

Conceived and designed the experiments: SK. Performed the experiments: TF SK. Analyzed the data: TF SK RI TT KS SM. Contributed reagents/materials/analysis tools: TF SK TM MT KH. Wrote the paper: TF SK.

References

1. Rose WC (1949) Amino acid requirements of man. Fed Proc 8: 546–552.
2. Seifter E, Rettura G, Barbul A, Levenson SM (1978) Arginine: an essential amino acid for injured rats. Surgery 84: 224–230.
3. Luiking YC, Deutz NE (2007) Exogenous arginine in sepsis. Crit Care Med 35: S557–563.
4. Schäffer MR, Tantry U, Gross SS, Wasserburg HL, Barbul A (1996) Nitric oxide regulates wound healing. J Surg Res 63: 237–240.
5. Schäffer MR, Efron PA, Thornton FJ, Klingel K, Gross SS, et al. (1997) Nitric oxide, an autocrine regulator of wound fibroblast synthetic function. J Immunol 158: 2375–2381.
6. Tan B, Yin Y, Kong X, Li P, Li X, et al (2010) L-Arginine stimulates proliferation and prevents endotoxin-induced death of intestinal cells. Amino Acids 38: 1227–1235.
7. Kim JY, Burghardt RC, Wu G, Johnson GA, Spencer TE, et al. (2011) Select nutrients in the ovine uterine lumen. VII. Effects of arginine, leucine, glutamine, and glucose on trophectoderm cell signaling, proliferation, and migration. Biol Reprod 84: 62–69.
8. Martin P (1997) Wound healing–aiming for perfect skin regeneration. Science 276: 75–81.
9. Gurtner GC, Werner S, Barrandon Y, Longaker MT (2008) Wound repair and regeneration. Nature 453: 314–321.